US Army Corps of Engineers

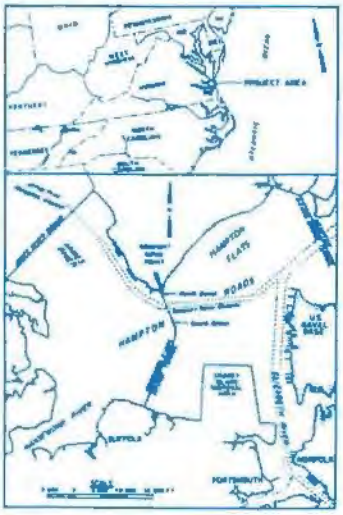

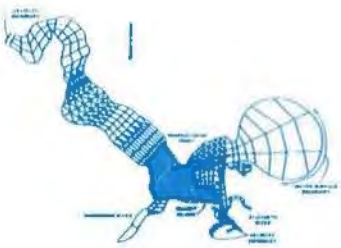

HYDRAULICS LABORATORY

TECHNICAL REPORT HL-88-8

LOWER JAMES RIVER CIRCULATION STUDY VIRGINIA, EVALUATION OF CRANEY ISLAND ENLARGEMENT ALTERNATIVES

by

Samuel B. Heltzel, Mitchell A. Granat

Hydraulics Laboratory

DEPARTMENT OF THE ARMY
Waterways Experiment Station, Corps of Engineers
PO Box 631, Vicksburg, Mississippi 39180-0631

April 1988
Final Report

Approved For Public Release; Distribution Unlimited

Prepared for Norfolk District Corps of Engineers
Norfolk, Virginia 23510-1096

Destroy this report when no longer needed. Do not return it to the originator.

The findings in this report are not to be construed as an official Department of the Army position unless so designated by other authorized documents.

The contents of this report are not to be used for advertising, publication, or promotional purposes. Citation of trade names does not constitute an official endorsement or approval of the use of such commercial products.

Unclassified

SECURITY CLASSIFICATION OF THIS PAGE

REPORT DOCUMENTATION PAGE

Form Approved OMB No. 0704-0188

1a. REPORT SECURITY CLASSIFICATION Unclassified	1b. RESTRICTIVE MARKINGS
2a. SECURITY CLASSIFICATION AUTHORITY	3. DISTRIBUTION/AVAILABILITY OF REPORT Approved for public release; distribution unlimited.
2b. DECLASSIFICATION/DOWNGRADING SCHEDULE	
4. PERFORMING ORGANIZATION REPORT NUMBER(S) Technical Report HL-88-8	5. MONITORING ORGANIZATION REPORT NUMBER(S)
6a. NAME OF PERFORMING ORGANIZATION USAEWES Hydraulics Laboratory 6b. OFFICE SYMBOL (If applicable) WESHE-E	7a. NAME OF MONITORING ORGANIZATION
6c. ADDRESS (City, State, and ZIP Code) PO Box 631 Vicksburg, MS 39180-0631	7b. ADDRESS (City, State, and ZIP Code)
8a. NAME OF FUNDING/SPONSORING ORGANIZATION Norfolk District Corps of Engineers 8b. OFFICE SYMBOL (If applicable) CENAO-PL-R	9. PROCUREMENT INSTRUMENT IDENTIFICATION NUMBER
8c. ADDRESS (City, State, and ZIP Code) 803 Front Street Norfolk, VA 23510-1096	10. SOURCE OF FUNDING NUMBERS PROGRAM ELEMENT NO. / PROJECT NO. / TASK NO. / WORK UNIT ACCESSION NO.
11. TITLE (Include Security Classification) Lower James River Circulation Study, Virginia; Evaluation of Craney Island Enlargement Alternatives	
12. PERSONAL AUTHOR(S) Heltzel, Samuel B., Granat, Mitchell A.	
13a. TYPE OF REPORT Final report 13b. TIME COVERED FROM _____ TO _____	14. DATE OF REPORT (Year, Month, Day) April 1988 15. PAGE COUNT 72
16. SUPPLEMENTARY NOTATION Available from National Technical Information Service, 5285 Port Royal Road, Springfield, VA 22161.	
17. COSATI CODES FIELD / GROUP / SUB-GROUP	18. SUBJECT TERMS (Continue on reverse if necessary and identify by block number) Craney Island; Hydrodynamics; Sedimentation; Estuarine circulation; James River; Flow convergence; Numerical modeling

19. ABSTRACT (Continue on reverse if necessary and identify by block number)

This report presents results from the numerical model investigation whose primary objective was to assess general changes in circulation, currents, and sedimentation associated with six proposed alternative expansion geometries of the Craney Island confined disposal facility. An additional objective of the study was to assess the effects of each of the six alternative geometries on the reported estuarine circulation cell (flow convergence) off Hampton Flats and Newport News Point.

This numerical model investigation used the TABS-2 finite element numerical models RMA-2V for hydrodynamics and STUDH for sedimentation with a modified version of an existing numerical mesh of the Lower James River. Other information presently available regarding the estuarine circulation and flow convergence observed off Newport News Point and Hampton Flats was reviewed.

(Continued)

20. DISTRIBUTION/AVAILABILITY OF ABSTRACT ☒ UNCLASSIFIED/UNLIMITED ☐ SAME AS RPT. ☐ DTIC USERS	21. ABSTRACT SECURITY CLASSIFICATION Unclassified
22a. NAME OF RESPONSIBLE INDIVIDUAL	22b. TELEPHONE (Include Area Code) / 22c. OFFICE SYMBOL

DD Form 1473, JUN 86 *Previous editions are obsolete.* SECURITY CLASSIFICATION OF THIS PAGE

Unclassified

19. ABSTRACT (Continued).

With the exception of the Newport News Channel, results from the numerical hydrodynamic modeling indicated no plan to base velocity differences greater than ±0.06 fps at any of the critical areas of interest. Velocity differences greater than 0.10 fps were indicated for the Newport News Channel; channel plan velocities always exceeded base velocities with maximum ebb velocity differences greater than maximum flood velocity differences. Plans with northward extensions resulted in the largest increases. The greatest changes, less than 0.35 fps on ebb and 0.25 fps on flood, were indicated for plans A and B, the largest expansion alternatives also involving westward expansions.

Subtle localized circulation variations, generally within 16,000 ft adjacent to and north and northwest of Craney Island, were identified in base to plan comparison vector plots.

Results from the numerical sedimentation modeling showed that plan to base shoaling index values (plan-predicted sedimentation divided by base-predicted sedimentation) were all within 90 to 110 percent at the critical areas of interest. The Nansemond River entrance was the only area considered to demonstrate any distinct changes in base and plan sedimentation. Considering the existing low sedimentation in the critical areas examined, the indicated differences are well within ordinary field survey detection limits.

Alternatives A, D, and F may impact water quality characteristics as a result of a reduced circulation zone between the Craney Island extension and the mainland.

Appendix A contains general information on the finite element method. A brief description of RMA-2V and STUDH appears in Appendices B and C, respectively.

PREFACE

In March 1987, the Norfolk District Corps of Engineers requested that the US Army Engineer Waterways Experiment Station (WES) conduct an investigation to assess general changes in circulation, currents, and sedimentation associated with six proposed alternative expansion geometries of Craney Island, the confined dredged material disposal site located in the lower James River.

The study was conducted by personnel of the Hydraulics Laboratory, WES, under the general direction of Messrs. F. A. Herrmann, Jr., Chief of the Hydraulics Laboratory; R. A. Sager, Assistant Chief of the Hydraulics Laboratory; W. H. McAnally, Jr., Chief of the Estuaries Division; and W. D. Martin, Chief of the Estuarine Engineering Branch. The project was conducted by Messrs. S. B. Heltzel and M. A. Granat, Estuarine Engineering Branch. This report was prepared by Messrs. Heltzel and Granat and edited by Mrs. Marsha C. Gay of the Information Technology Laboratory, WES.

The valuable technical and nontechnical contributions of Mr. J. R. Melchor, Norfolk District Corps of Engineers, are gratefully acknowledged.

COL Dwayne G. Lee, CE, is the Commander and Director of WES. Dr. Robert W. Whalin is the Technical Director.

CONTENTS

CONVERSION FACTORS, NON-SI TO SI (METRIC) UNITS OF MEASUREMENTS

Non-SI units of measurement used in this report can be converted to SI (metric) units as follows:

Multiply	By	To Obtain
acres	4,046.873	square metres
cubic feet	0.02831685	cubic metres
cubic yards	0.7645549	cubic metres
feet	0.3048	metres

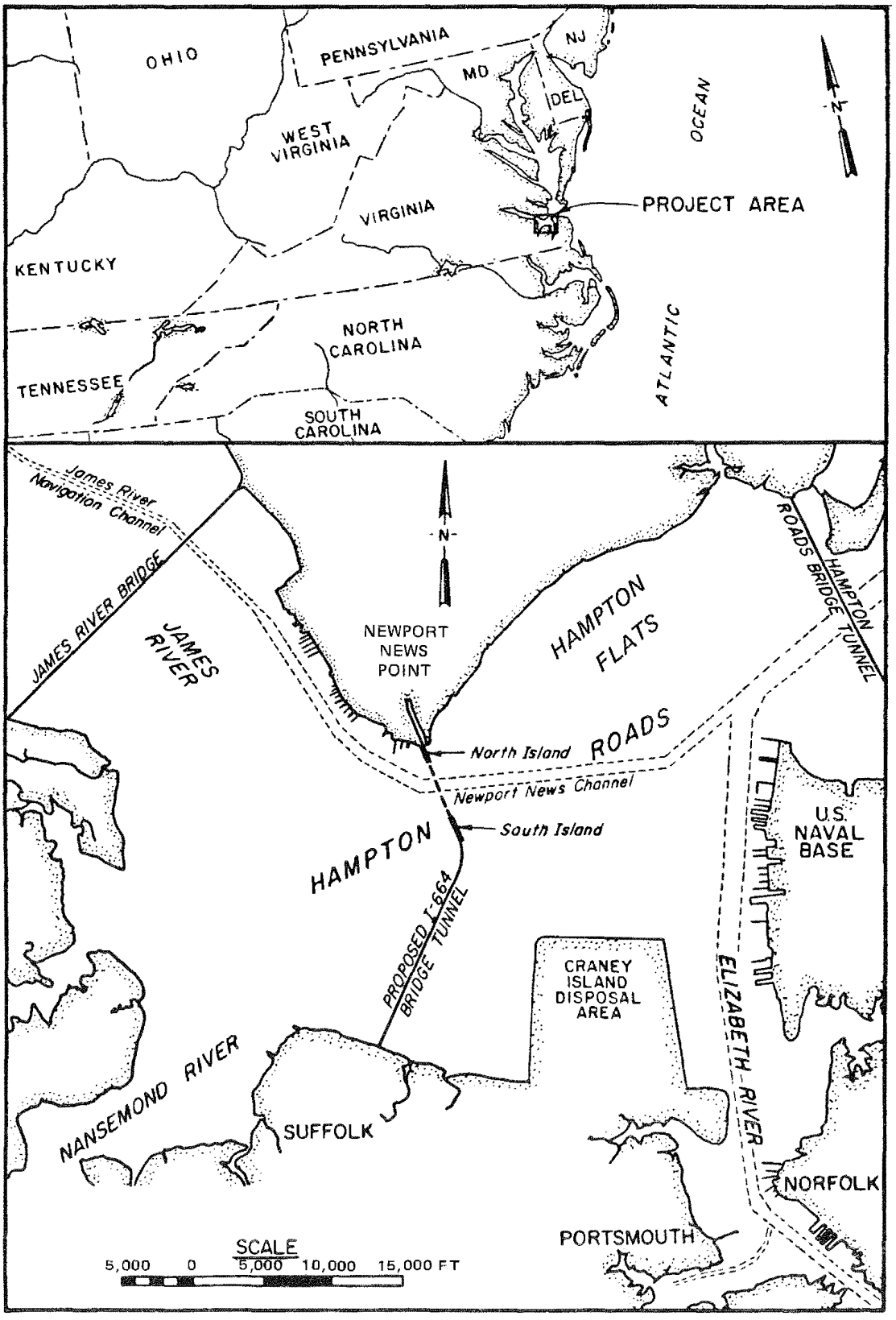

Figure 1. Project location

LOWER JAMES RIVER CIRCULATION STUDY, VIRGINIA
EVALUATION OF CRANEY ISLAND ENLARGEMENT ALTERNATIVES

PART I: INTRODUCTION

Background

1. The existing Craney Island disposal area is a 2,500-acre* confined disposal facility located near Norfolk, Virginia (Figure 1). Design plans for the facility were developed in the early 1940's, and construction was undertaken between 1954 and 1957. Several retaining dike elevation increases and the implementation of a management plan developed specifically for Craney Island (Palermo, Shields, and Hayes 1981) have greatly extended the useful life of the facility beyond initial expectations. At present, approximately 5 million cubic yards of predominately fine-grained maintenance dredged material from the channels and ports in the Hampton Roads area are annually disposed of in the facility.

2. Additional new work dredged material from the Norfolk Harbor and channels deepening and improvement project will also be placed into Craney Island. This new work dredged material will greatly reduce the storage capacity and active life of Craney Island. An expansion of the existing site or the development of an alternate site will be necessary to contain future new work and maintenance dredged material once the existing disposal site has reached its capacity. Six alternative expansion configurations for Craney Island are presently being considered by the Norfolk District Corps of Engineers.

3. An assessment of the impact of each alternative on circulation and sedimentation in the lower James River was undertaken as a preliminary planning level task. Other concurrent tasks included analyses to determine the storage capacity and active dredged material disposal life of each of the proposed alternatives and development of preliminary guidelines for management

---

* A table of factors for converting non-SI to SI (metric) units of measurement is presented on page 3.

of the new areas* and an evaluation of the required retaining dike geotechnical engineering characteristics (stability, constructibility, and cost) for each alternative (Spigolon and Fowler 1987).

Purpose

4. The primary objective of the present study was to use available numerical models to assess general changes in circulation, currents, and sedimentation associated with each of the six proposed alternative expansion geometries of Craney Island. An additional objective of the study was to assess the effects of each of the six alternative geometries on the reported estuarine circulation cell (flow convergence) off Hampton Flats and Newport News Point.

Scope

5. The numerical modeling portion of this study was designed to address relative alternative-induced changes in overall hydrodynamics and to assess relative sedimentation changes in four specific critical zones of interest. The primary focus was circulation and sedimentation in relatively low velocity areas, so the cohesive version of a numerical sediment code was used since it more directly reflected circulation and suspended sediment transport. Figure 2 illustrates the James River study area with the four zones of interest highlighted: Area A, the entrance to Willoughby Bay; Area B, the Hampton Flats; Area C, the entrance to the Nansemond River; and Area D, Burwell Bay.

6. The circulation cell off Newport News Point and Hampton Flats was addressed using results from the numerical model study, comparison with surface current pattern mosaics from earlier physical model investigations** of the James River, review of a recent investigation of the area (Byrne et al. 1987) conducted by the Virginia Institute of Marine Science (VIMS), and a

---

* G. F. Goforth. 1986. "Disposal Life Evaluation of Alternative Expansion Configurations for Craney Island Disposal Facility," Draft Report, US Army Engineer Waterways Experiment Station, Vicksburg, Miss.

** N. J. Brogdon, Jr., and W. H. Bobb. 1967. "Effects of Proposed Waterfront Developments at Newport News Point on Tides, Currents, Salinities, and Shoaling," Draft Report, US Army Engineer Waterways Experiment Station, Vicksburg, Miss.

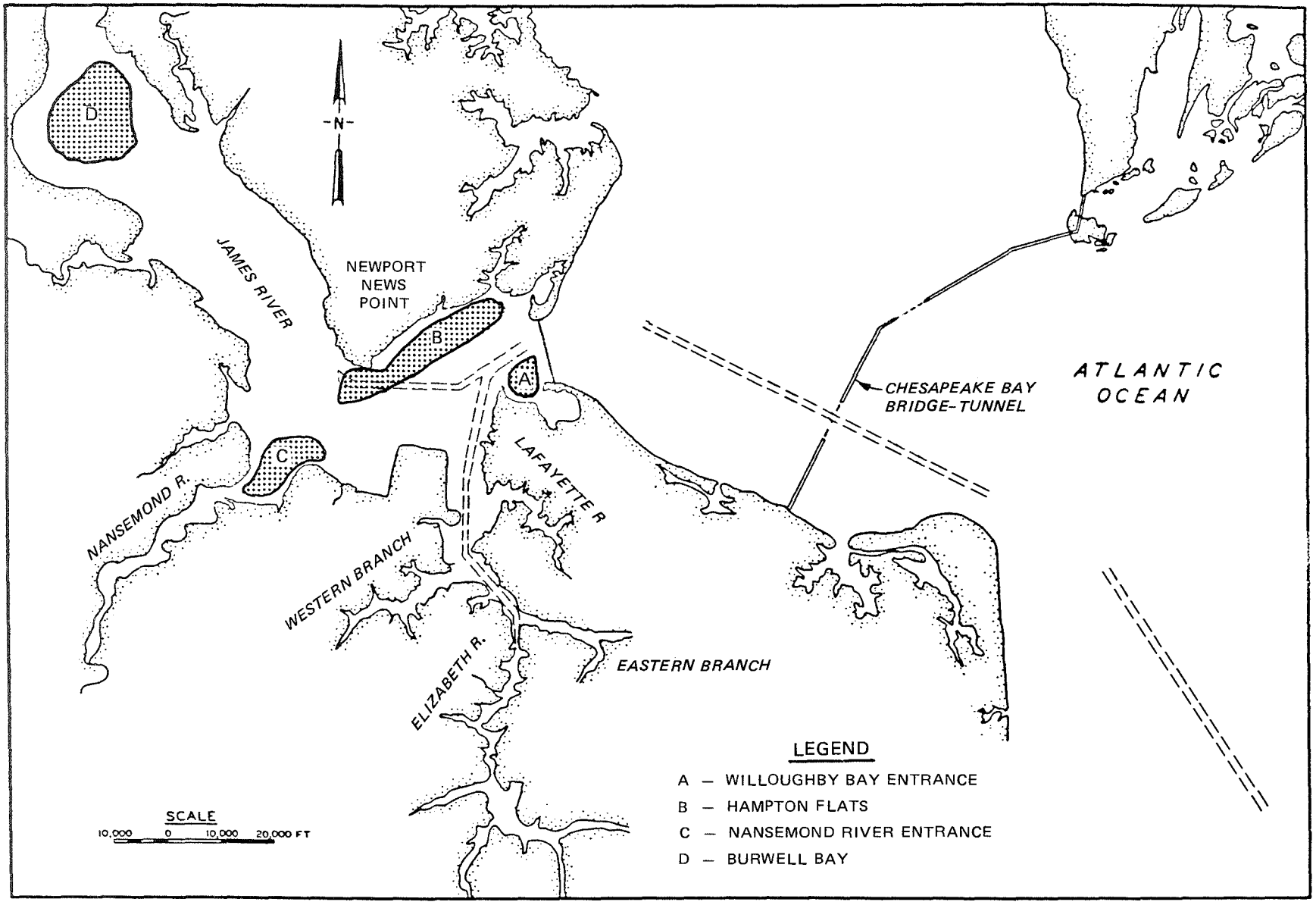

Figure 2. Critical sedimentation zones of interest

review* of a limited field data set collected by the US Army Engineer Waterways Experiment Station (WES) during a relatively low freshwater discharge period during July 1986.

* S. B. Heltzel. 1986 (2 Sep). "Memorandum for Record: Interim Report - Norfolk Harbor Long-Term Disposal Study," US Army Engineer Waterways Experiment Station, Vicksburg, Miss.

PART II: NUMERICAL MODELING APPROACH

The Numerical Models

7. The Corps numerical modeling system, Open-Channel Flow and Sedimentation, TABS-2 (Thomas and McAnally 1985), was used in this investigation. The two primary finite element numerical model codes used were A Two-Dimensional Model for Free Surface Flows (RMA-2V) and Sediment Transport in Unsteady Two-Dimensional Flows, Horizontal Plane (STUDH). Both codes employ the finite element method to solve the depth-integrated governing equations. Appendix A contains general information on the finite element method. A brief description of RMA-2V and STUDH appears in Appendices B and C, respectively.

Lower James River Computational Meshes

8. The computational mesh used during this investigation was a modified version of the mesh developed for the I-664 bridge tunnel crossing study (Heltzel, in preparation). Modifications to this mesh included (a) revising the schematization around Craney Island by adding additional elements to incorporate the six Craney Island enlargement alternatives, (b) extending the mesh into lower Chesapeake Bay to improve modeling of hydrodynamic and sedimentation processes in the Willoughby Bay area, and (c) effectively doubling the mesh resolution in the critical zones of Burwell Bay, the Nansemond River entrance, and Newport News Point/Hampton Flats area. All of the conditions tested included the completed I-664 bridge tunnel crossing and the 55-ft Newport News and Norfolk Harbor channels.

9. The basic revised mesh, presented in Figure 3, contains 2,326 nodes and 806 elements. This mesh incorporates all six alternative geometries to eliminate the possibility of required mesh resolution refinement between conditions as a possible cause for anomalous plan variations in hydrodynamic or sedimentation results. An enlarged view of the Craney Island area illustrating the schematization used for each of the proposed enlargement alternatives is provided in Figure 4. The highlighted areas in each schematization indicate the elements that were deleted from the computational space for each of the conditions considered. During testing, the boundary of each mesh conformed to the new geometry for each of the respective alternatives. Figure 5

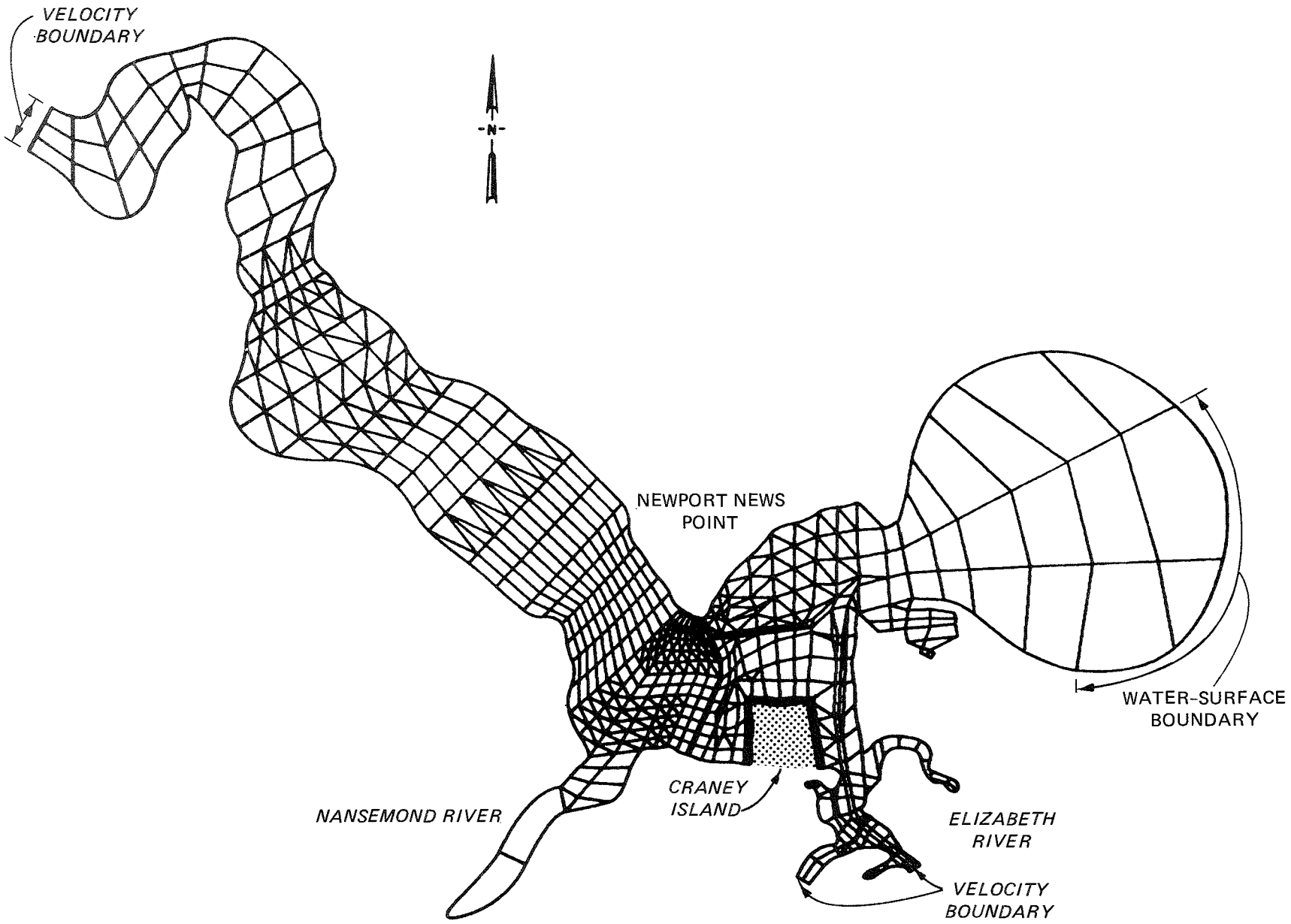

Figure 3. Numerical model mesh for lower James River-Craney Island study

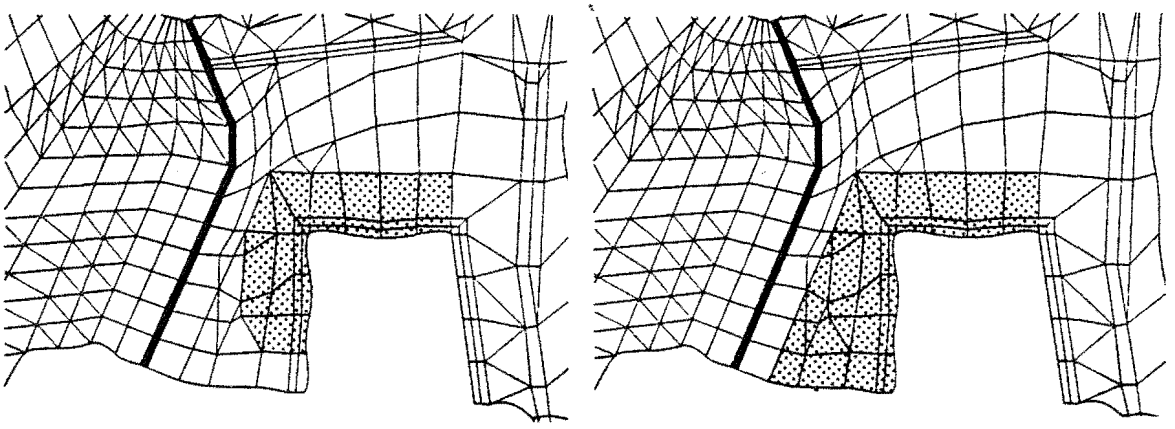

a. Plan A

b. Plan B

c. Plan C

d. Plan D

e. Plan E

f. Plan F

NOTE: SHADED AREAS REPRESENT ALTERNATIVE EXTENSIONS.

Figure 4. Mesh schematization of Craney Island enlargement alternatives

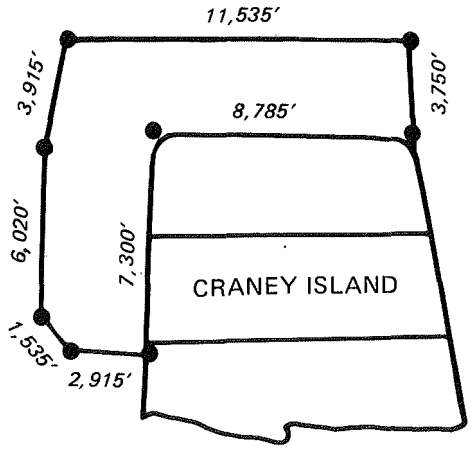

a. Plan A

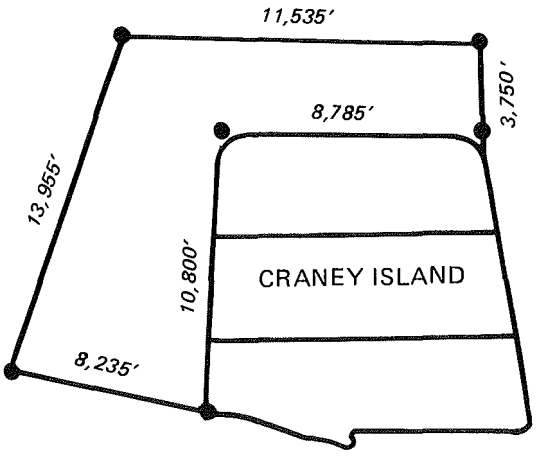

b. Plan B

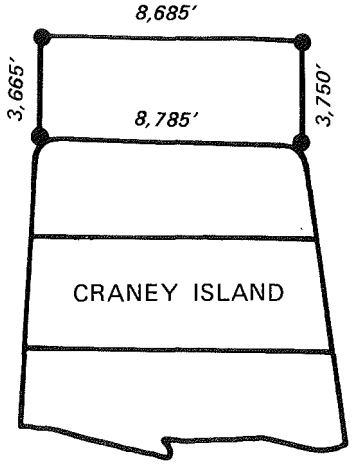

c. Plan C

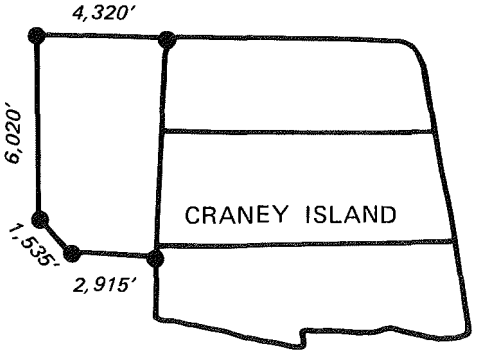

d. Plan D

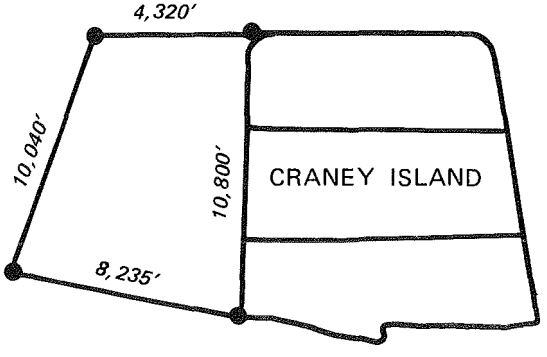

e. Plan E

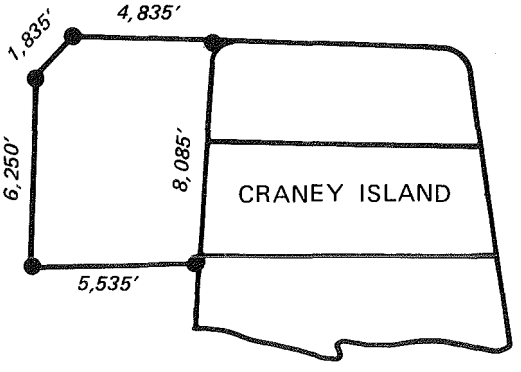

f. Plan F

Figure 5. Dimensions of Craney Island enlargement alternatives

provides the actual plan dimensions for each of the analyzed Craney Island extensions.

Testing Conditions

10. Physical model data collected in the Chesapeake Bay hydraulic model during the Norfolk Harbor and channels deepening study (Richards and Morton 1983) were used to develop boundary conditions for the numerical hydrodynamic model. Physical model water-surface elevation data were used to generate boundary forcing functions at the lower Chesapeake Bay numerical model boundary, and depth-averaged physical model velocity data were used at the upper James and Elizabeth River numerical model boundaries.

11. The same hydrodynamic coefficients and modeling procedures developed during the I-664 bridge tunnel crossing study (Heltzel, in preparation) and the numerical Norfolk Harbor and channels deepening study (Berger et al. 1985) were used during this investigation. Water-surface elevation and velocity data from several interior locations within the revised mesh were compared to data from the I-664 investigation to ensure that the revised schematization and boundary conditions did not alter hydrodynamic characteristics. Cohesive sediment coefficients and modeling procedures developed during the I-664 and Norfolk investigations were similarly employed during the Craney Island study. These parameters provided results that compared well with the limited field sedimentation information and the suspended sediment concentrations reported for the areas of interest.

12. A series of base (revised mesh without any Craney Island expansion) numerical model sensitivity studies were undertaken prior to final base and plan testing to determine the boundary condition that produced the maximum sedimentation in the areas of interest. As indicated in the numerical Norfolk Harbor and channels deepening study (Berger et al. 1985), and as confirmed by these sensitivity studies, the mean range tide (2.5 ft at Old Point Comfort) and long-term average James River freshwater discharge condition (8,900 cfs combined total James River tributary freshwater inflow) generally resulted in maximum sedimentation rates. The mean range tide and long-term average freshwater discharge conditions were used as the forcing functions for final testing of the base and plan configurations. It should be noted that the ocean salinity was maintained at 32.5 ppt during the physical model study.

PART III: ESTUARINE CIRCULATION AND FLOW CONVERGENCE: HAMPTON FLATS AND NEWPORT NEWS POINT

13. This section summarizes information presently available regarding the estuarine circulation and flow convergence observed off Newport News Point and the Hampton Flats. This summary is based on previous studies* conducted on the James River physical model at WES, Vicksburg, Mississippi; a recent detailed investigation conducted by VIMS (Byrne et al. 1987) evaluating potential impacts associated with the development of an island (New Port Island) on Hampton Flats; and a limited supplemental field data collection effort conducted by WES during the period 22-24 July 1986.**

James River Physical Model Investigations

14. Several physical model dye studies in the late 1960's (as summarized in Byrne et al. 1987) investigated James River circulation patterns to determine optimum oyster larvae release locations in an attempt to reestablish the lower James River oyster beds. These early investigations demonstrated the existence and importance of the estuarine net nontidal flow characteristics of the lower James River.

15. Surface current pattern mosaics taken during several of the physical model studies provide excellent visual documentation of the existing surface circulation patterns. Figure 6 illustrates a set of photographs taken over a 4-hour period (2.4 min in the model) during a study sponsored by the City of Newport News to specifically investigate effects of proposed waterfront developments at Newport News Point on tides, currents, salinities, and shoaling. The study was conducted during the period November 1966 to March 1967, and the results were documented by Brogdon and Bobb (1967).*

16. Each photograph illustrates the trajectory of surface confetti during a simulated 5-min period (3 sec in the model). A strobe light activated at the end of each exposure dotted the confetti streaks, identifying the flow direction. The indicated times are referenced to the specific hour after the moon's transit over the entrance to Chesapeake Bay (the 76th meridian).

---

* Brogdon and Bobb, op. cit.
** Heltzel, op. cit.

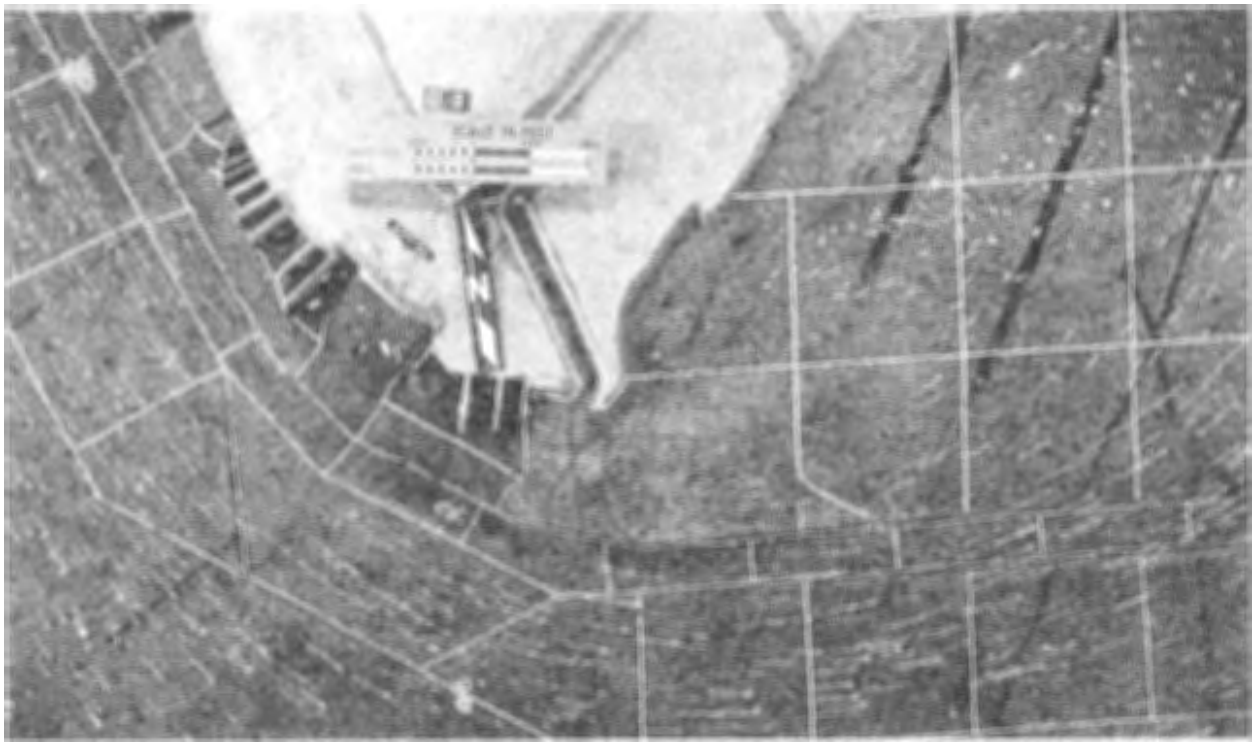

a. Hour 3

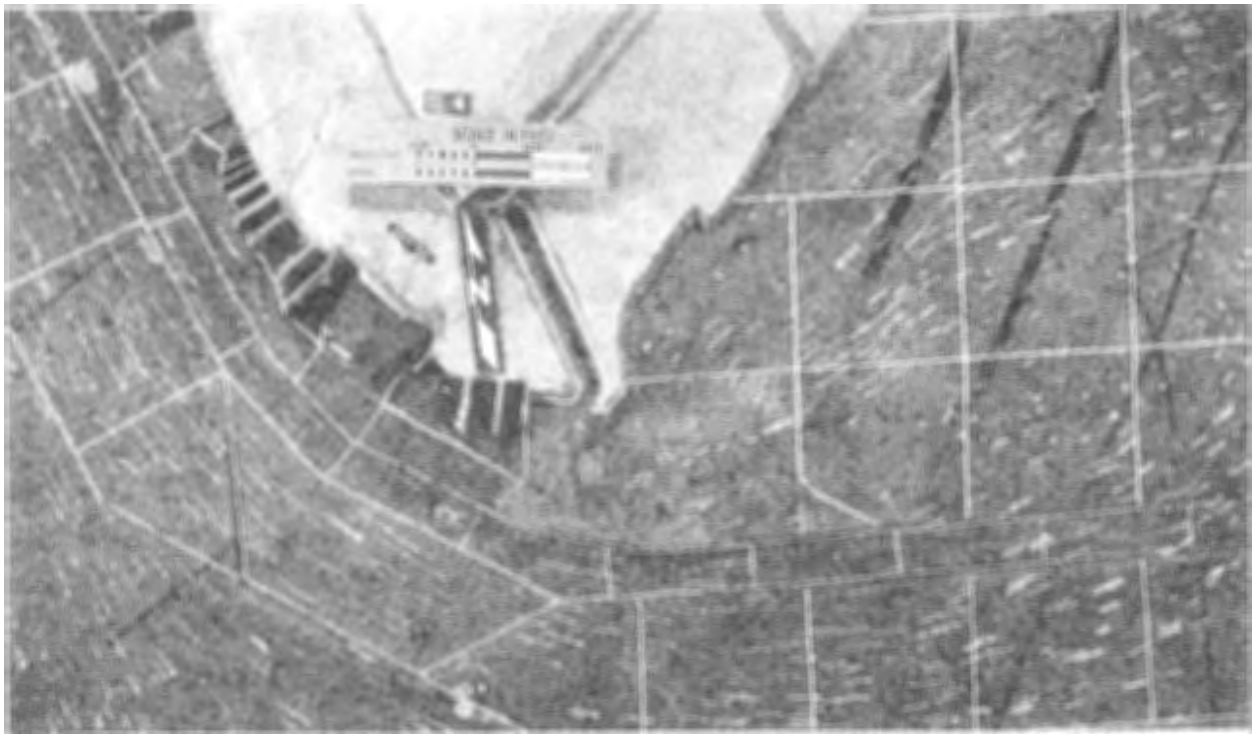

b. Hour 4

Figure 6. Surface currents, hours 3-6 (from Brogdon and Bobb, op. cit.) (Continued)

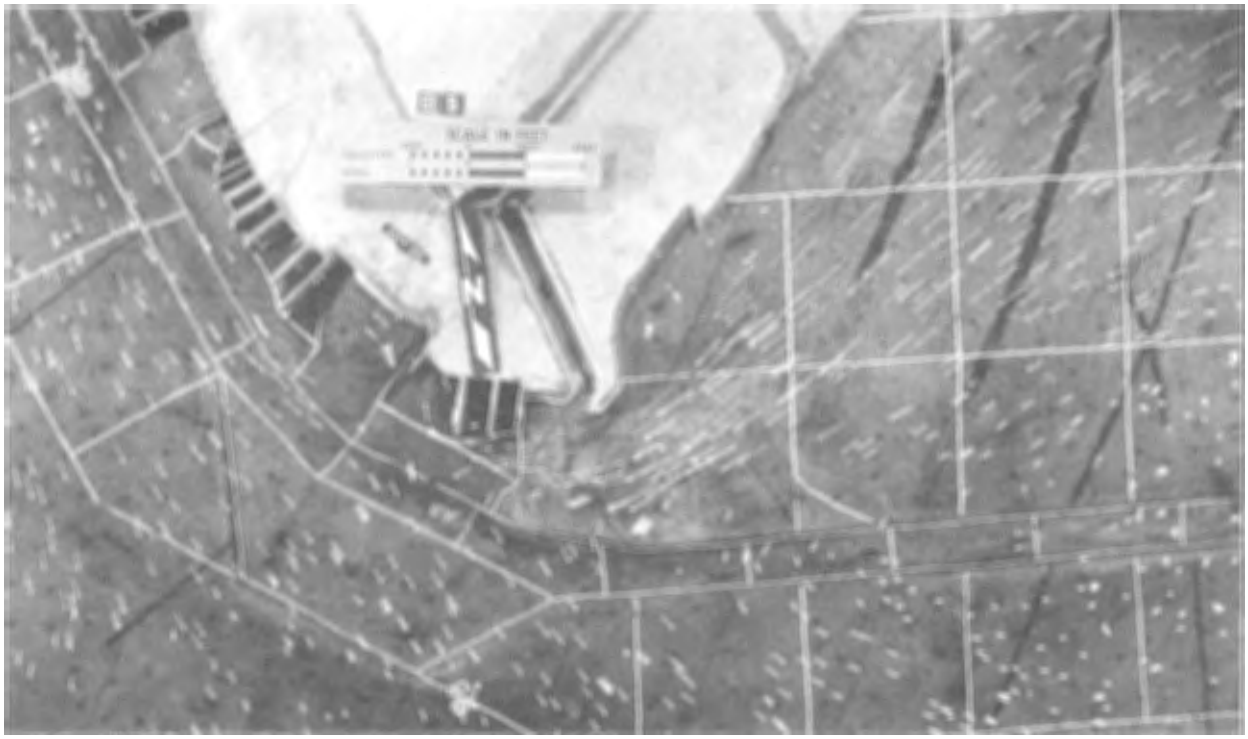

c. Hour 5

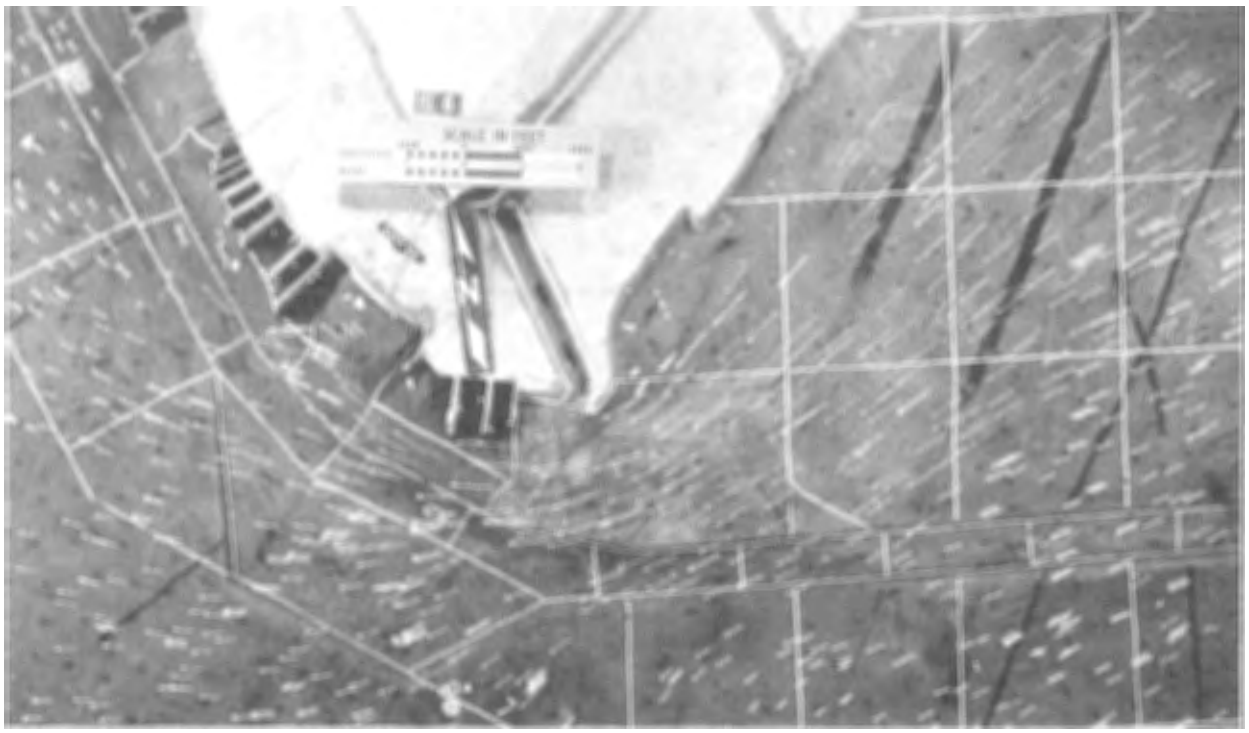

d. Hour 6

Figure 6. (Concluded)

The illustrated base condition included the proposed 35-ft channel from Newport News to Richmond and the proposed enlargement of Newport News Channel and anchorages. The boundary conditions included a 2.5-ft mean tide range condition at Hampton Roads, a Chesapeake Bay sump salinity of 24.2 ppt, and the long-term average freshwater inflow of 7,500 cfs for the James at Richmond, 1,000 cfs for the Appomattox, 300 cfs for the Chickahominy, and 700 cfs for the Nansemond which included the discharges of the Warwick, Pagan, Chuckatuck, and Elizabeth rivers.

17. As indicated in Figure 6, an early onset of the flood current over the Hampton Flats area began at hour 3 while the flow upstream of Newport News Point and south of Hampton Flats was still at strength of ebb. As demonstrated at hour 4, flood flow over Hampton Flats was fully developed while flows west of Newport News Point and in Newport News Channel were still ebbing. The flood current was not fully developed in Newport News Channel and west of Newport News Point until hour 6. Similar circulation patterns were demonstrated in the other physical model studies.

New Port Island Investigation

18. The New Port Island study recently completed by VIMS (Byrne et al. 1987) was an extensive multitasked investigation conducted to evaluate potential lower James River marine resources impacts associated with the development of New Port Island, a recreational/port facility, to be located on Hampton Flats. A major emphasis of this study was the estuarine circulation off Newport News Point, its effects on oyster larvae transport, and the potential impacts associated with various alternative configurations for the proposed island.

19. The VIMS study concluded that the flow convergence off Newport News Point, described as a frontal system, was a persistent phenomenon expected to occur during times of flood current under normal tidal range, freshwater inflow, and meteorological conditions. The flow convergence was said to be the result of geometry-induced local phase (time of arrival) differences between initial flood currents on Hampton Flats and Newport News Channel and ebbing flows west of Newport News Point. The local salinity distribution was said to be another essential factor to the formation of the front. During development of the flow convergence, the currents on Hampton Flats, and later

in the Newport News Channel, began to flood while the currents west of Newport News Point were still ebbing. The study also concluded that the depth transition at Newport News Point enhanced and stabilized the location of the convergence zone. Dye studies demonstrated that the surface floodwaters downstream of the convergence zone were transported to depths of 13 to 16 ft upstream of the convergence zone.

WES Supplemental Field Survey

20. WES conducted a limited field survey* in the lower James River on 22-24 July 1986 to acquire additional supplemental field data during a preliminary stage in the development of a three-dimensional James River modeling effort. Four boats were used to collect vertical velocity and salinity data at 13 stations during a complete 13-hr tidal cycle on 22 and 24 July. Data were collected at five locations in the vertical and at approximately half-hour intervals where station spacing permitted.

21. Environmental conditions were not representative of normal conditions in the lower James River. The freshwater discharge of approximately 1,000 cfs was well below the long-term average condition. In addition, strong winds were blowing and gusting from the east and southeast during the survey effort. The boat located at Newport News Point was unable to complete the entire tidal cycle survey due to high wave conditions; data were collected only during the later stages of ebb and the early stages of flood, the predicted period of time for the convergence phenomenon. As confirmed by the vertical salinity data, these conditions resulted in a reduced stratification.

22. Instantaneous middepth velocities were analyzed for the 13 stations during this period of time. These data demonstrated the early flood on Hampton Flats relative to the Newport News Channel station. Tidally averaged bottom velocities generally illustrated net upstream movement onto the Hampton Flats and net downstream movement in the Newport News Channel. The velocities averaged over depth and then over the tidal cycle illustrated the same general trends with some magnitude changes. The existence of this circulation and the convergence phenomenon, despite the unfavorable conditions for its formation (low freshwater discharge and high winds and waves), clearly demonstrates its

---

* Heltzel, op. cit.

persistence. The acquired data did not confirm or disprove the plunging current concept discussed in the VIMS report.

PART IV: MODELING RESULTS AND DISCUSSION

Hydrodynamic Impacts

23. Localized and subtle base to plan hydrodynamic differences were indicated. Hydrodynamic vector plots for maximum ebb* (hr 14.00) and maximum flood (hr 20.00) conditions in the lower James River for each of the plan conditions are printed in red in Plates 1-12. The corresponding base condition is printed in black on each plate. Except for the Craney Island extension area, where only base vectors occur, the plan velocity was identical to base conditions (i.e., when red plan vectors exactly overlay black base vectors, only the black vector is visible). Closeup hydrodynamic vector plots for the Newport News/Hampton Flats area for the period around slack before flood (hr 15.00, 16.00, and 17.00) for each of the plan conditions are printed in red in Plates 13-18. These plots illustrate the Hampton Flats circulation cell and the convergence zone for each plan condition. Again, the corresponding base circulation is printed in black on each plot. Each of the vector plots is based on a regular grid pattern that uses the finite element shape functions and the calculated nodal velocity vectors.

24. Subtle localized variations, generally within 16,000 ft adjacent to and north and northwest of Craney Island, are indicated on the vector plots comparing the plan conditions to the base condition. Plans A-C (Plates 1-6), which all involve northward Craney Island extensions, appear to illustrate the largest hydrodynamic impacts. Plans A and B, which also involve westward extensions, illustrate the largest changes. Some of the indicated variation may be the result of small plan to base phase shifts or simply numerical noise.

25. The vector plots provide an excellent visual presentation of the circulation for each condition; however, quantifying variations between the various plans is difficult from these plots. Figure 7 illustrates the locations of 13 nodes that were examined in detail to summarize the actual

---

* As in the physical model investigations, the indicated times are referenced to the moon's transit over the entrance to Chesapeake Bay (the 76th meridian). A repetitive 12.42-hr tidal cycle was used in the numerical model runs; i.e., hr 13.00 (the first time-step in cycle 2) corresponds to hr 0.58 of the first tidal cycle.

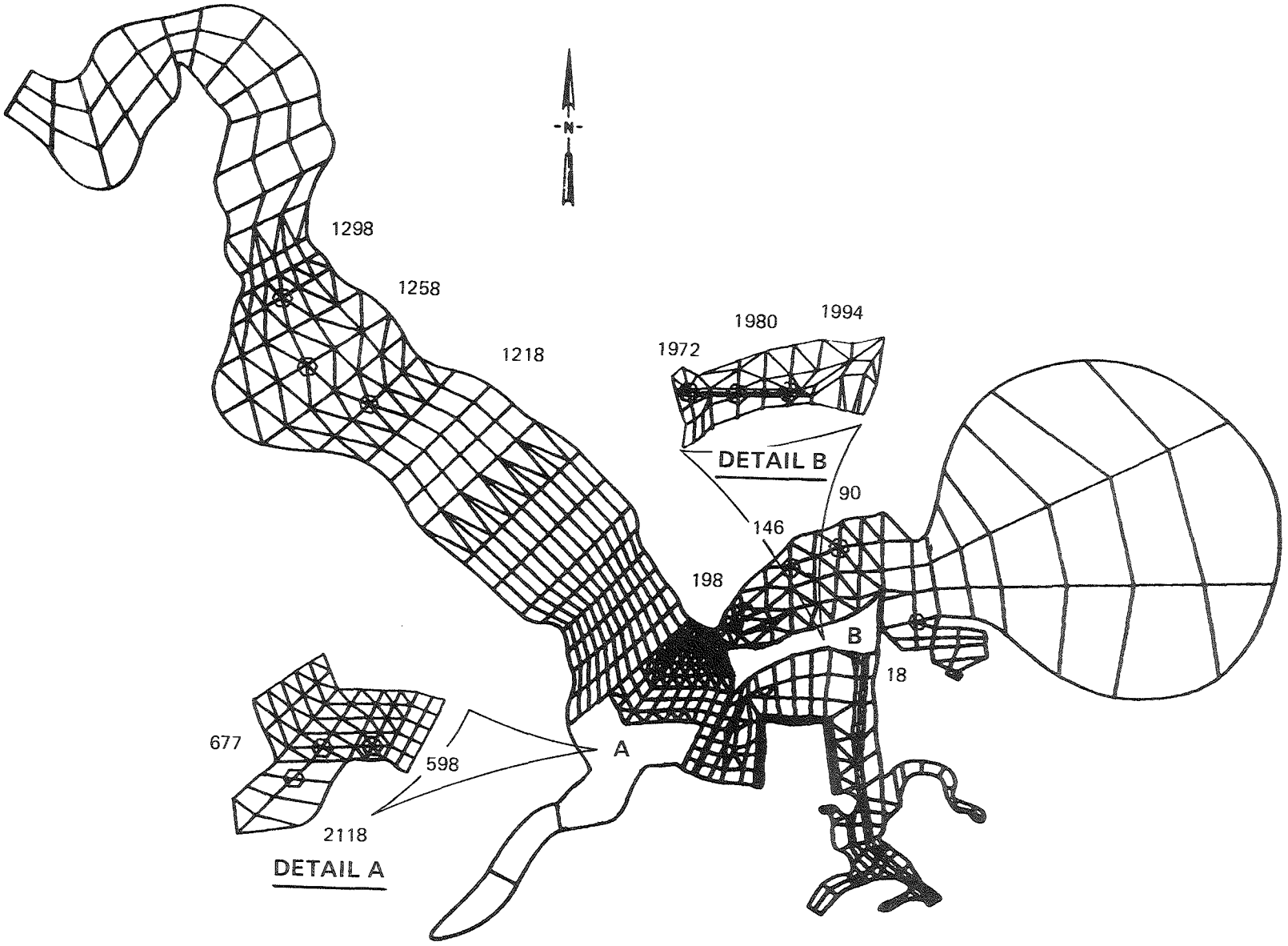

Figure 7. Numerical model nodes examined in detail

differences in magnitude between the velocities of the base condition and each of the plan conditions. In the order listed, node 18 is located in the center of the Willoughby Bay zone of interest (Area A); nodes 90, 146, and 198 are located in Hampton Flats (Area B); nodes 598, 677, and 2118 are located in the Nansemond River zone of interest (Area C); nodes 1218, 1258, and 1298 are located in the Burwell Bay zone of interest (Area D); and nodes 1994, 1980, and 1972 are located in the thalweg of the Newport News Channel.

26. Table 1 provides the maximum ebb and flood magnitudes for base conditions at each node location and the magnitude differences for each of the plan conditions. As indicated, with the exception of Newport News Channel, all maximum velocity differences (plan magnitude minus base magnitude) at the examined critical areas of interest were generally within field and model confidence limits and never greater than 0.06 fps from base conditions. Noticeable plan to base differences (velocity differences greater than 0.10 fps) were indicated for the Newport News Channel nodes. Channel plan velocities always exceeded base velocities with maximum ebb velocity differences greater than maximum flood velocity differences. As expected, the plans with northward extensions resulted in the largest increases. The greatest changes, less than 0.35 fps on ebb and 0.25 fps on flood (Table 1), were indicated for plans A and B, the largest expansion alternatives which also involved westward expansions.

27. Plates 19-28 illustrate selected node time-history plots of water-surface elevations and ebb and flood velocity magnitudes. A node from the center of each of the critical areas and one from the Newport News Channel was selected from each plan condition for comparison to the base condition. Similar plots for other node locations are available, but are not included in this report. The first few hours of each model run should not be used for comparison or analysis since they may be affected by model spin-up conditions.

28. The time-history plots provide an excellent means of illustrating actual phase (time of arrival) and magnitude differences at specific node locations over the tidal cycle. As previously addressed, with the exception of the Newport News Channel, only subtle base to plan hydrodynamic variations were identified. The subtle phase shifts illustrated may be partially responsible for the some of the variations indicated on the vector plots.

29. Results from the depth-integrated numerical model demonstrate that the formation of the circulation cell off Newport News and Hampton Flats will

continue under all of the alternative plans examined. This circulation cell is the result of the early onset of the flood currents over Hampton Flats associated with bathymetric shielding of the ebb currents over the flats by Newport News Point. This large-scale geometry-induced phase difference existed during all of the plans tested.

30. The differences indicated in the time-history and vector plots are subtle and indicate the impacts to be localized, within 16,000 ft of Craney Island (see paragraph 24), with no impacts identified to the general estuarine circulation outside of this region. The bathymetric shielding, combined with the depth transition as described in the VIMS study (Byrne et al. 1987) and summarized in paragraph 19, has the effect of stabilizing the location of the convergence zone.

31. Potential impacts to the reported frontal system, a three-dimensional phenomenon, should not be quantified with the information from the present investigation. The following generalizations can be made, however, based upon the available information and present estuarine experience. Hydrodynamic impacts to the general three-dimensional circulation will be small, if any, and will be extremely difficult to measure. Alternatives with northward Craney Island expansions will have the greatest potential to affect the three-dimensional circulation processes.

Sedimentation Impacts

32. Sedimentation rates are generally sensitive to subtle variations in circulation characteristics. Small changes in hydrodynamic processes are usually amplified in the sedimentation responses. Sedimentation comparisons therefore provide an excellent means of quantitatively assessing overall base to plan impacts.

33. For reporting purposes, the predicted shoaling volume for each element in the zone of interest was combined to estimate yearly shoaling rates for each zone. Table 2 provides a summary of the plan-predicted sedimentation divided by the base-predicted sedimentation, the plan to base shoaling index value, for the four critical areas of interest for each of the six alternative plans. Based on available field data, shoaling rates in each of these areas are generally low (less than 0.5 ft/year), and the indicated shoaling index values are generally well within normal hydrographic survey detection limits.

34. Of the four zones examined, the Nansemond River entrance, Area C, is the only zone considered to demonstrate any distinct change in base to plan sedimentation. It should be stressed that even these variations are rather subtle, especially considering the generally low sedimentation rates. Plans A, B, and C, which all involve northward extensions of Craney Island, resulted in reduced sedimentation in the Nansemond area for the alternative conditions. The largest sedimentation change, about a 9 percent reduction in shoaling, was indicated for plan C, the alternative that involved expansion only to the north.

35. Plans D, E, and F, which involve only westward extensions of Craney Island, resulted in increased sedimentation in the Nansemond area. Plan F resulted in the largest increase, about a 7 percent increase from the base shoaling rate. The second largest increase, about 4 percent, was indicated for plan D. It is interesting to note that none of alternatives A, D, nor F extends to the mainland (Figure 4), allowing additional sluggish circulation between the disposal site and the mainland. Plan E extends to the mainland. Although this alternative encompasses a larger area than either plans F or D, it appears to have a reduced impact on sedimentation. An additional consideration associated with plans A, D and F is a potential impact on water quality associated with reduced circulation between the mainland and the disposal site (Plates 1 and 2, 7 and 8, and 11 and 12).

PART V: CONCLUSIONS

36. No plan to base velocity differences greater than ±0.06 fps were identified at any of the four critical areas of interest. With the exception of the Newport News Channel, only localized and subtle base to plan velocity differences were indicated. Plan to base magnitude increases greater than ±0.10 fps were identified in the Newport News Channel. The greatest increases, less than 0.35 fps on ebb and 0.25 fps on flood, were indicated for plans A and B, which involved both northward and westward Craney Island extensions.

37. Subtle localized circulation variations were identified in base to plan comparison vector plots. When these variations occurred, they were generally within 16,000 ft north and northwest of Craney Island. In some instances, these variations were associated with slight hydrodynamic phase shifts.

38. Plan to base shoaling index values (plan-predicted sedimentation divided by base-predicted sedimentation) for all conditions were well within hydrographic survey detection limits. The Nansemond River entrance was the only zone that demonstrated any distinct change in plan to base sedimentation. These variations were rather subtle, less than ±10 percent.

39. Plans A, B, and C, involving extensions to the north, resulted in reduced sedimentation within the Nansemond zone. The largest change, about a 9 percent reduction in sedimentation, was indicated for plan C, the alternative that involved only northward extension.

40. Increased sedimentation within the Nansemond zone was indicated for plans D, E, and F, which involve only westward extensions of Craney Island. The largest increases were for plans D and F (about 4 and 7 percent, respectively), Craney Island extensions which do not extend to the mainland.

41. Alternate plans A, D, and F may impact water quality characteristics as a result of a reduced circulation zone between the Craney Island extension and the mainland.

42. Formation of the circulation cell off Newport News and Hampton Flats will continue under all of the alternatives examined. The general location of the convergence zone was also unaffected.

43. Potential three-dimensional circulation impacts to the reported frontal phenomenon cannot be quantified with the available two-dimensional

numerical model results. Alternatives with northward expansions have the greatest potential for any hydrodynamic impact, although even these impacts are felt to be small relative to the capability to measure them in the field.

REFERENCES

Ariathurai, R., MacArthur, R. C., and Krone, R. B. 1977 (Oct). "Mathematical Model of Estuarial Sediment Transport," Technical Report D-77-12, US Army Engineer Waterways Experiment Station, Vicksburg, Miss.

Berger, R. C., Jr., Heltzel, S. B., Athow, R. F., Jr., Richards, D. R., and Trawle, M. J. 1985 (Mar). "Norfolk Harbor and Channels Deepening Study; Sedimentation Investigation, Chesapeake Bay Hydraulic Model Investigation," Technical Report HL-83-13, Report 2, US Army Engineer Waterways Experiment Station, Vicksburg, Miss.

Byrne, R. J., Kuo, A. Y., Mann, R. L., Brubaker, J. M., Ruzecki, E. P., Hyer, P. V., Diaz, R. J., and Posenau, J. H. 1987 (Feb). "New Port Island: An Evaluation of Potential Impacts on Marine Resources of the Lower James River and Hampton Roads," Special Report in Applied Marine Science and Ocean Engineering No. 283, Virginia Institute of Marine Science, Gloucester Point, Va.

Desai, C. S. 1979. Elementary Finite Element Method, Prentice Hall, Englewood Cliffs, N. J.

Heltzel, S. B. "I-664 Bridge Tunnel Study, Virginia; Sedimentation and Circulation Investigation" (in preparation), US Army Engineer Waterways Experiment Station, Vicksburg, Miss.

Krone, R. B. 1962 (Jun). "Flume Studies of Transport of Sediment in Estuarial Shoaling Processes," Final Report, Hydraulics Engineering Research Laboratory, University of California, Berkeley, Calif.

Norton, W. R., and King, I. P. 1977 (Feb). "Operating Instructions for the Computer Program RMA-2V," Resource Management Associates, Lafayette, Calif.

Palermo, M. R., Shields, F. D., and Hayes, D. F. 1981 (Dec). "Development of a Management Plan for Craney Island Disposal Area," Technical Report EL-81-11, US Army Engineer Waterways Experiment Station, Vicksburg, Miss.

Partheniades, E. 1962. "A Study of Erosion and Deposition of Cohesive Soils in Salt Water," Ph.D. Dissertation, University of California, Berkeley, Calif.

Richards, D. R., and Morton, M. R. 1983 (Jun). "Norfolk Harbor and Channels Deepening Study; Physical Model Results; Chesapeake Bay Hydraulic Model Investigation," Technical Report HL-83-13, Report 1, US Army Engineer Waterways Experiment Station, Vicksburg, Miss.

Spigolon, S. J., and Fowler, J. 1987. "Geotechnical Feasibility Study Replacement or Extension of the Craney Island Disposal Area, Norfolk, Virginia," Miscellaneous Paper GL-87-9, US Army Engineer Waterways Experiment Station, Vicksburg, Miss.

Stewart, J. P., Daggett, L. L., and Athow, R. F. 1985 (May). "Impact of Proposed Runway Extension at Little Rock Municipal Airport on Water-Surface Elevations and Navigation Conditions in Arkansas River," Miscellaneous Paper HL-85-3, US Army Engineer Waterways Experiment Station, Vicksburg, Miss.

Thomas, W. A., and McAnally, W. H., Jr. 1985 (Aug). "User's Manual for the Generalized Computer Program System; Open-Channel Flow and Sedimentation, TABS-2; Main Text and Appendices A through O," Instruction Report HL-85-1, US Army Engineer Waterways Experiment Station, Vicksburg, Miss.

Zienkiewicz, O. C. 1971. The Finite Element Method in Engineering Science, McGraw-Hill, London.

Table 1

Velocity Changes at Selected Nodes (Plan Minus Base)

Area	Node No.	Base Maximum, fps		Change, fps											
				Plan A		Plan B		Plan C		Plan D		Plan E		Plan F	
		Ebb	Flood	Ebb	Flood	Ebb	Flood	Ebb	Flood	Ebb	Flood	Ebb	Flood	Ebb	Flood
Willoughby Bay (Area A)	18	0.68	0.70	-0.02	-0.02	-0.03	-0.03	-0.02	-0.02	-0.01	-0.01	-0.01	-0.02	-0.01	-0.01
Hampton	90	0.58	0.60	-0.04	-0.01	-0.02	-0.01	-0.01	0.00	-0.01	0.00	-0.01	-0.01	-0.01	-0.01
Flats	146	0.63	0.55	0.02	0.02	0.01	0.02	0.02	0.02	0.01	0.01	0.00	0.00	0.01	0.01
(Area B)	198	0.82	0.65	0.00	0.06	0.00	0.06	0.00	0.04	0.04	0.00	-0.05	0.00	-0.04	0.00
Nansemond	598	0.43	0.54	-0.04	-0.01	-0.03	-0.01	-0.01	0.00	-0.02	0.00	-0.02	0.00	-0.03	-0.01
River	677	0.52	0.73	-0.01	-0.04	-0.01	-0.04	0.00	-0.02	0.00	-0.02	0.00	-0.02	0.00	-0.02
(Area C)	2118	0.67	0.71	-0.02	-0.03	-0.02	-0.03	-0.02	-0.01	-0.02	-0.01	-0.02	-0.01	-0.02	-0.01
Burwell	1218	1.43	1.26	-0.03	0.00	-0.03	0.00	-0.02	0.00	-0.02	0.01	-0.02	0.01	-0.02	0.01
Bay	1258	1.13	1.39	-0.01	-0.03	-0.01	-0.03	0.00	-0.02	0.00	-0.01	0.00	-0.01	0.00	-0.01
(Area D)	1298	1.24	1.32	0.02	-0.02	0.02	-0.02	0.02	-0.01	0.02	0.00	0.02	-0.01	0.02	-0.01
Newport	1994	1.10	1.06	0.10	0.04	0.09	0.03	0.12	0.06	0.00	-0.01	-0.01	-0.01	0.00	-0.01
News	1980	1.30	1.22	0.27	0.17	0.25	0.16	0.17	0.15	0.05	0.00	0.04	-0.01	0.05	0.00
Channel	1972	2.05	1.24	0.33	0.23	0.32	0.22	0.18	0.12	0.15	0.04	0.14	0.04	0.16	0.05

Table 2

Shoaling Index (Plan/Base)

Area	Plan A	Plan B	Plan C	Plan D	Plan E	Plan F
A	0.99	0.99	0.99	0.99	0.99	0.99
B	1.01	1.01	1.01	1.00	1.01	1.01
C	0.93	0.94	0.91	1.04	1.03	1.07
D	1.00	0.99	1.00	1.00	0.99	0.99

PLATES

PLATE 1

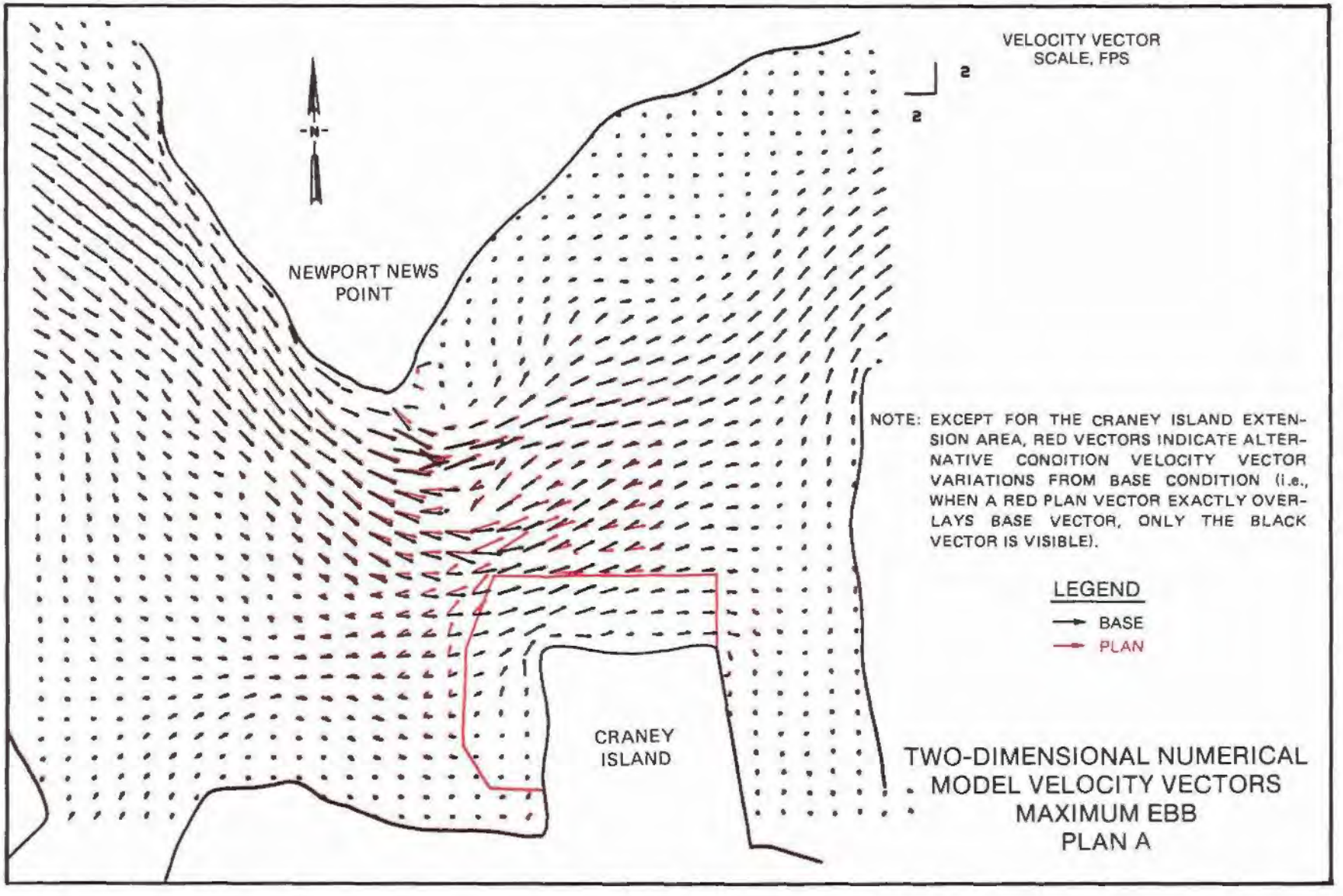
VELOCITY VECTOR
SCALE, FPS
2
2
-N-
NEWPORT NEWS
POINT
CRANEY
ISLAND
NOTE: EXCEPT FOR THE CRANEY ISLAND EXTENSION AREA, RED VECTORS INDICATE ALTERNATIVE CONDITION VELOCITY VECTOR VARIATIONS FROM BASE CONDITION (i.e., WHEN A RED PLAN VECTOR EXACTLY OVERLAYS BASE VECTOR, ONLY THE BLACK VECTOR IS VISIBLE).
LEGEND
BASE
PLAN
TWO-DIMENSIONAL NUMERICAL
MODEL VELOCITY VECTORS
MAXIMUM EBB
PLAN A

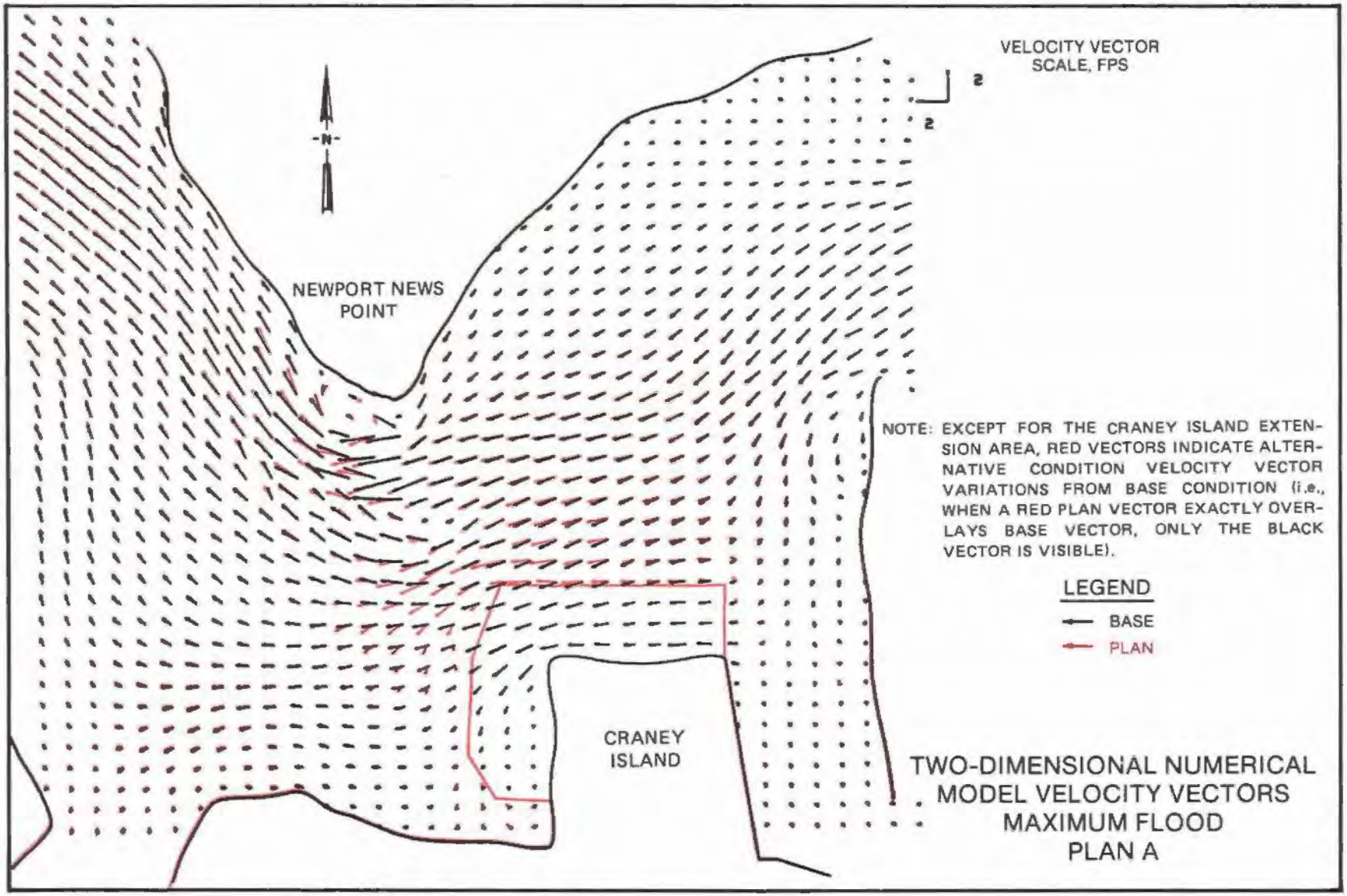
VELOCITY VECTOR
SCALE, FPS
2
2
N
NEWPORT NEWS
POINT
CRANEY
ISLAND
NOTE: EXCEPT FOR THE CRANEY ISLAND EXTENSION AREA, RED VECTORS INDICATE ALTERNATIVE CONDITION VELOCITY VECTOR VARIATIONS FROM BASE CONDITION (i.e., WHEN A RED PLAN VECTOR EXACTLY OVERLAYS BASE VECTOR, ONLY THE BLACK VECTOR IS VISIBLE).
LEGEND
BASE
PLAN
TWO-DIMENSIONAL NUMERICAL
MODEL VELOCITY VECTORS
MAXIMUM FLOOD
PLAN A

PLATE 2

PLATE 3

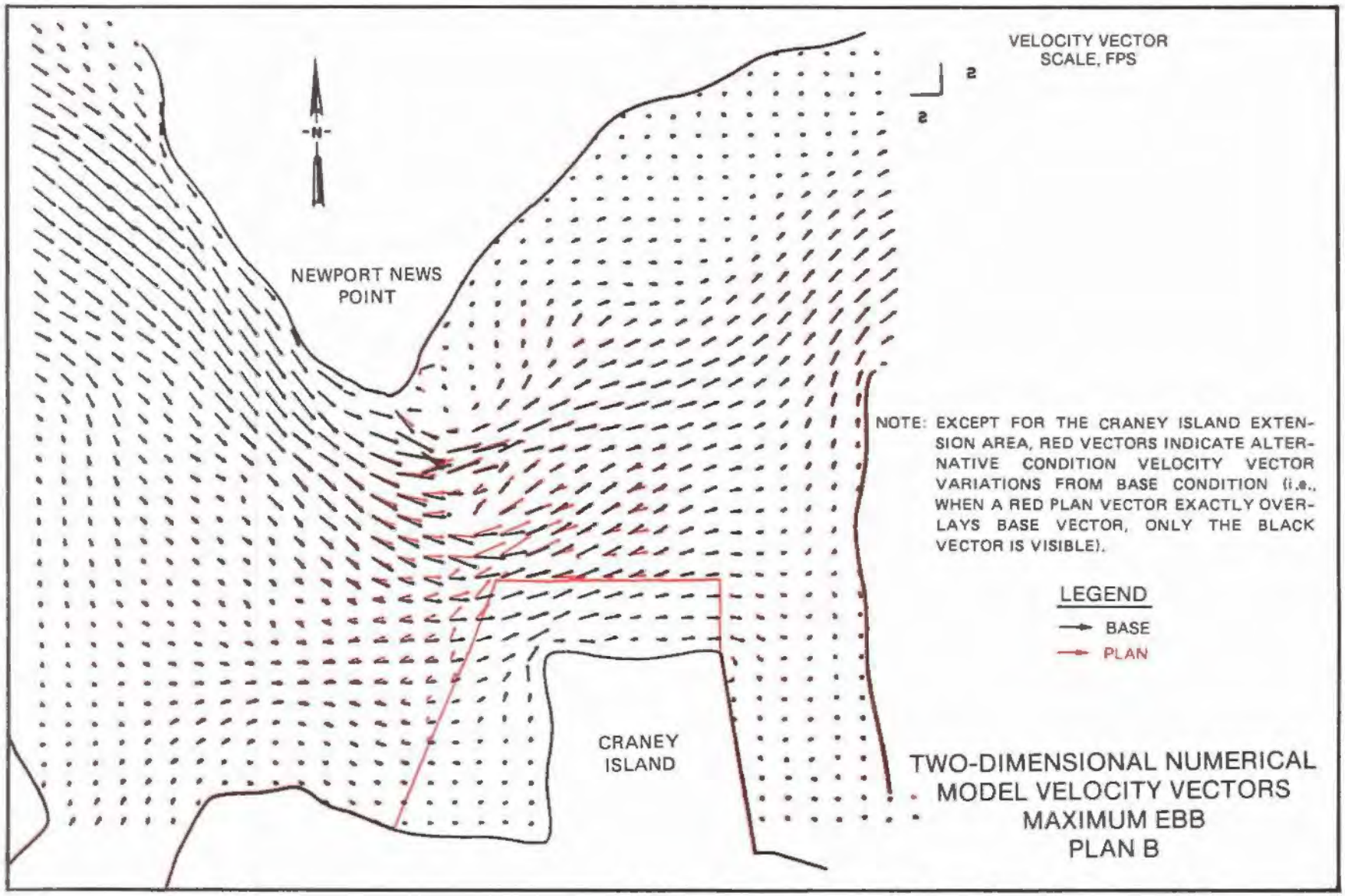
VELOCITY VECTOR
SCALE, FPS
2
2
N
NEWPORT NEWS
POINT
CRANEY
ISLAND
NOTE: EXCEPT FOR THE CRANEY ISLAND EXTENSION AREA, RED VECTORS INDICATE ALTERNATIVE CONDITION VELOCITY VECTOR VARIATIONS FROM BASE CONDITION (i.e., WHEN A RED PLAN VECTOR EXACTLY OVERLAYS BASE VECTOR, ONLY THE BLACK VECTOR IS VISIBLE).
LEGEND
BASE
PLAN
TWO-DIMENSIONAL NUMERICAL
MODEL VELOCITY VECTORS
MAXIMUM EBB
PLAN B

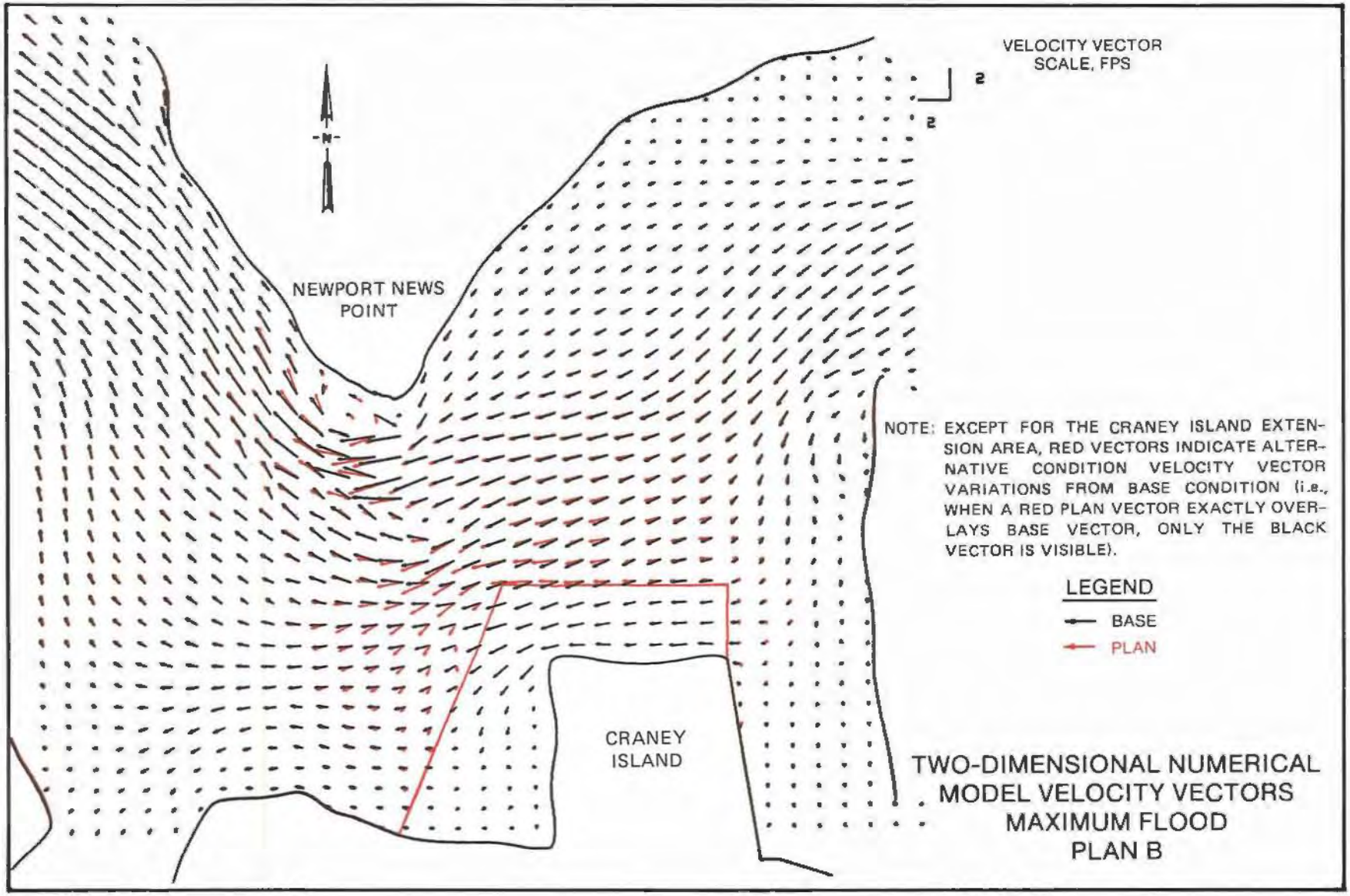
VELOCITY VECTOR
SCALE, FPS
2
2
N
NEWPORT NEWS
POINT
CRANEY
ISLAND
NOTE: EXCEPT FOR THE CRANEY ISLAND EXTENSION AREA, RED VECTORS INDICATE ALTERNATIVE CONDITION VELOCITY VECTOR VARIATIONS FROM BASE CONDITION (i.e., WHEN A RED PLAN VECTOR EXACTLY OVERLAYS BASE VECTOR, ONLY THE BLACK VECTOR IS VISIBLE).
LEGEND
BASE
PLAN
TWO-DIMENSIONAL NUMERICAL
MODEL VELOCITY VECTORS
MAXIMUM FLOOD
PLAN B

PLATE 4

PLATE 5

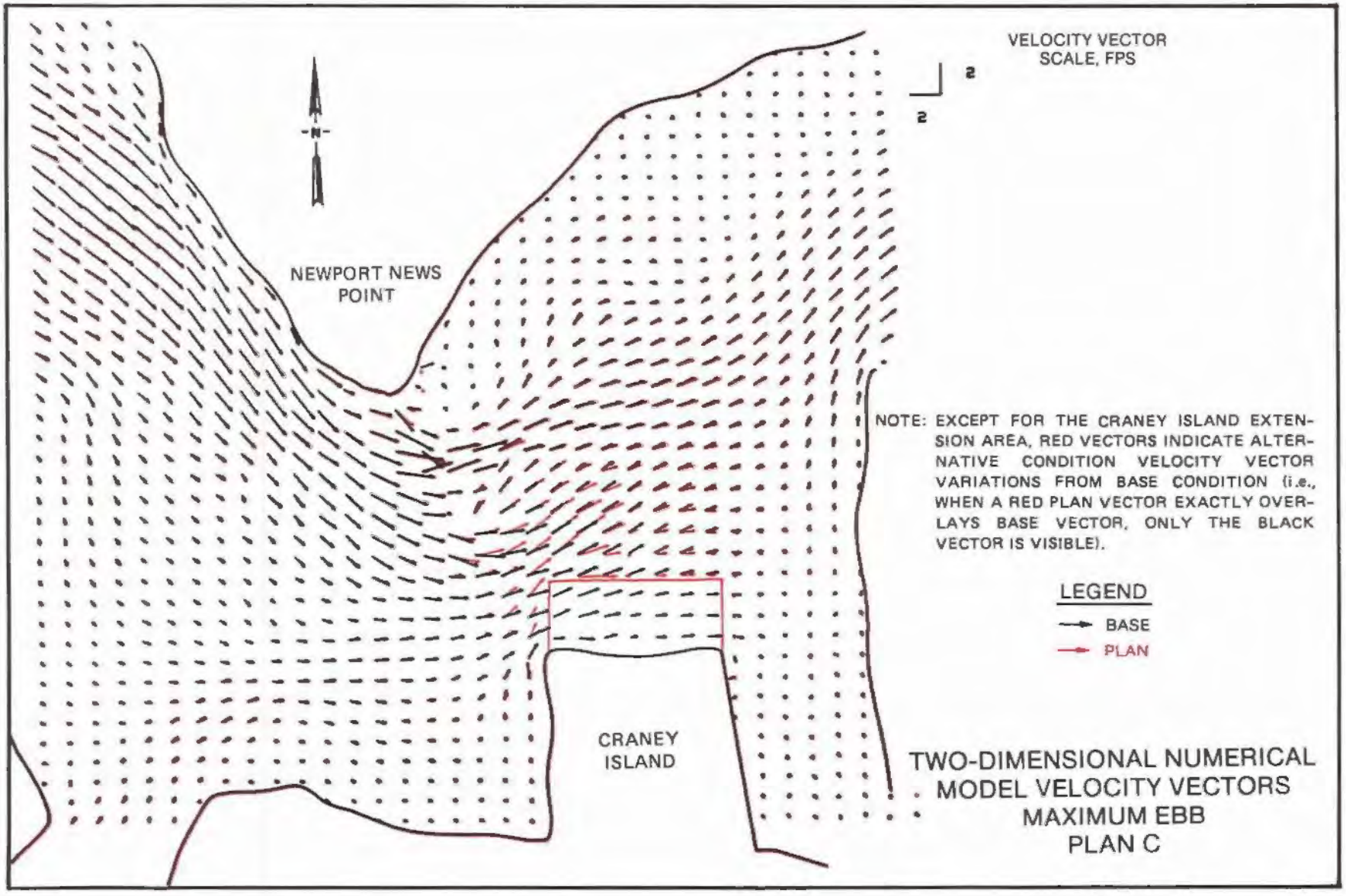
VELOCITY VECTOR
SCALE, FPS
2
2
N
NEWPORT NEWS
POINT
CRANEY
ISLAND
NOTE: EXCEPT FOR THE CRANEY ISLAND EXTENSION AREA, RED VECTORS INDICATE ALTERNATIVE CONDITION VELOCITY VECTOR VARIATIONS FROM BASE CONDITION (i.e., WHEN A RED PLAN VECTOR EXACTLY OVERLAYS BASE VECTOR, ONLY THE BLACK VECTOR IS VISIBLE).
LEGEND
BASE
PLAN
TWO-DIMENSIONAL NUMERICAL
MODEL VELOCITY VECTORS
MAXIMUM EBB
PLAN C

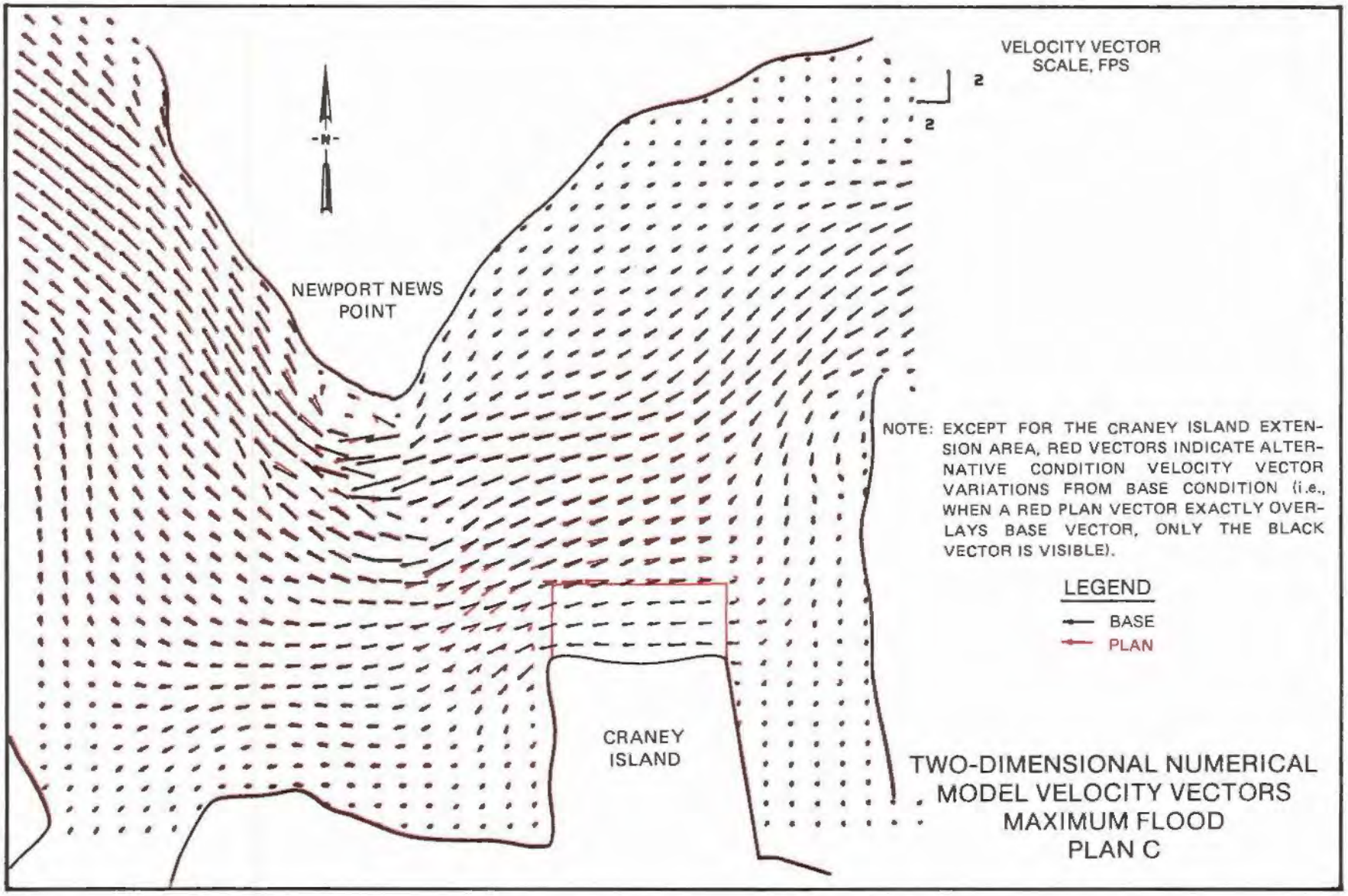
VELOCITY VECTOR
SCALE, FPS
2
2
N
NEWPORT NEWS
POINT
CRANEY
ISLAND
NOTE: EXCEPT FOR THE CRANEY ISLAND EXTENSION AREA, RED VECTORS INDICATE ALTERNATIVE CONDITION VELOCITY VECTOR VARIATIONS FROM BASE CONDITION (i.e., WHEN A RED PLAN VECTOR EXACTLY OVERLAYS BASE VECTOR, ONLY THE BLACK VECTOR IS VISIBLE).
LEGEND
BASE
PLAN
TWO-DIMENSIONAL NUMERICAL
MODEL VELOCITY VECTORS
MAXIMUM FLOOD
PLAN C

PLATE 6

PLATE 7

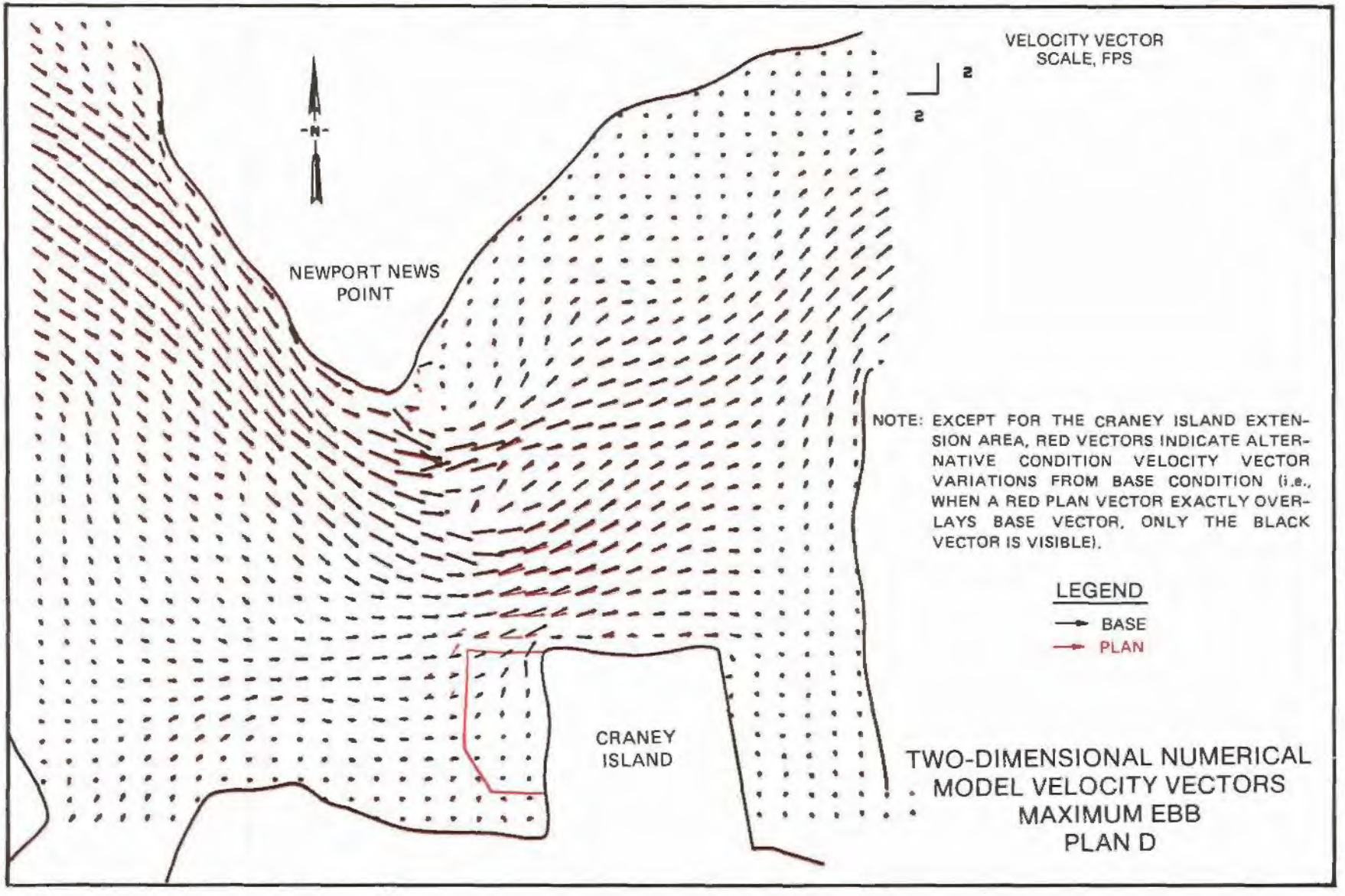
VELOCITY VECTOR
SCALE, FPS
2
2
N
NEWPORT NEWS
POINT
CRANEY
ISLAND
NOTE: EXCEPT FOR THE CRANEY ISLAND EXTENSION AREA, RED VECTORS INDICATE ALTERNATIVE CONDITION VELOCITY VECTOR VARIATIONS FROM BASE CONDITION (i.e., WHEN A RED PLAN VECTOR EXACTLY OVERLAYS BASE VECTOR, ONLY THE BLACK VECTOR IS VISIBLE).
LEGEND
BASE
PLAN
TWO-DIMENSIONAL NUMERICAL
MODEL VELOCITY VECTORS
MAXIMUM EBB
PLAN D

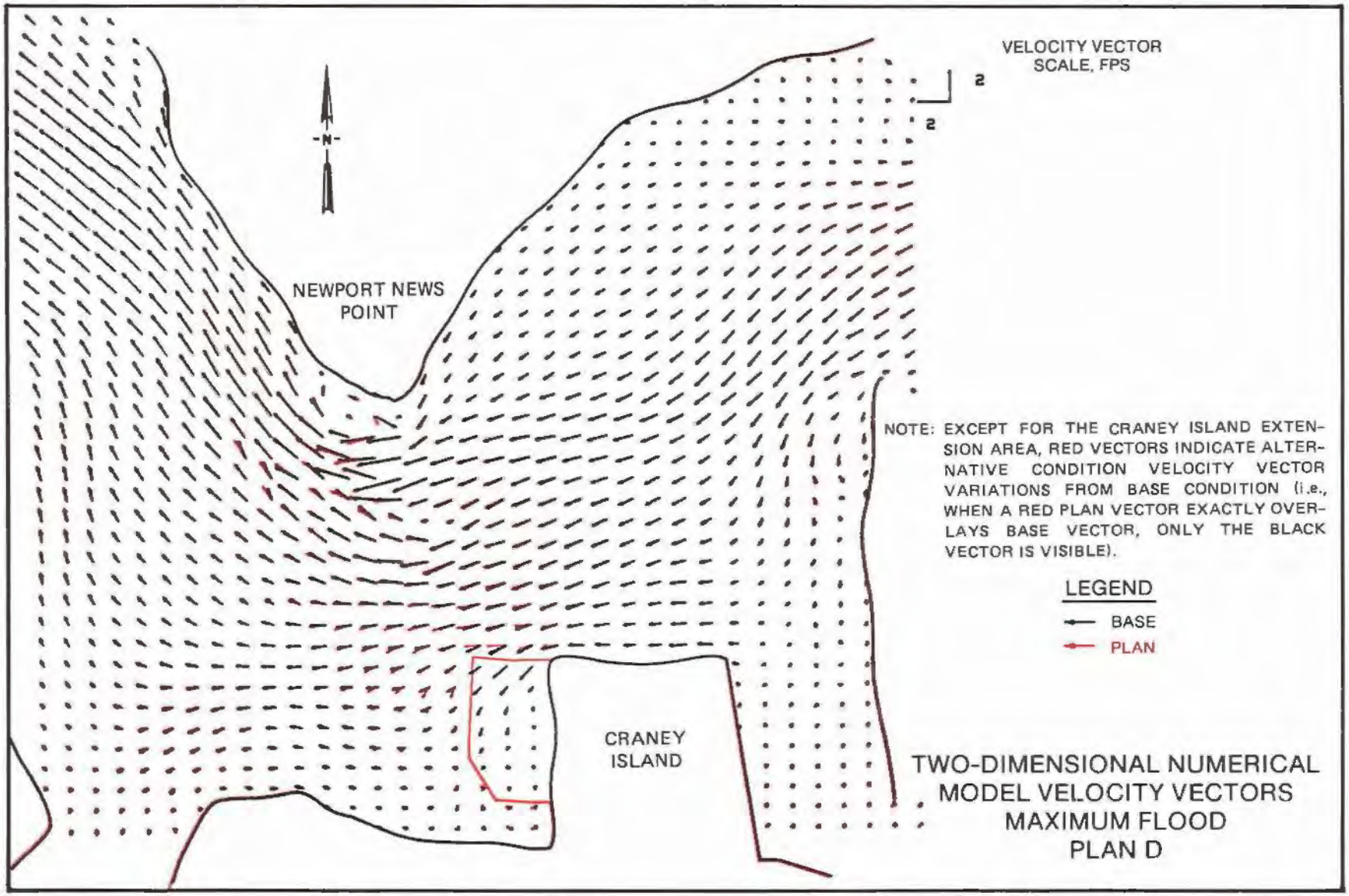
VELOCITY VECTOR
SCALE, FPS
2
2
N
NEWPORT NEWS
POINT
CRANEY
ISLAND
NOTE: EXCEPT FOR THE CRANEY ISLAND EXTENSION AREA, RED VECTORS INDICATE ALTERNATIVE CONDITION VELOCITY VECTOR VARIATIONS FROM BASE CONDITION (i.e., WHEN A RED PLAN VECTOR EXACTLY OVERLAYS BASE VECTOR, ONLY THE BLACK VECTOR IS VISIBLE).
LEGEND
BASE
PLAN
TWO-DIMENSIONAL NUMERICAL
MODEL VELOCITY VECTORS
MAXIMUM FLOOD
PLAN D

PLATE 8

PLATE 9

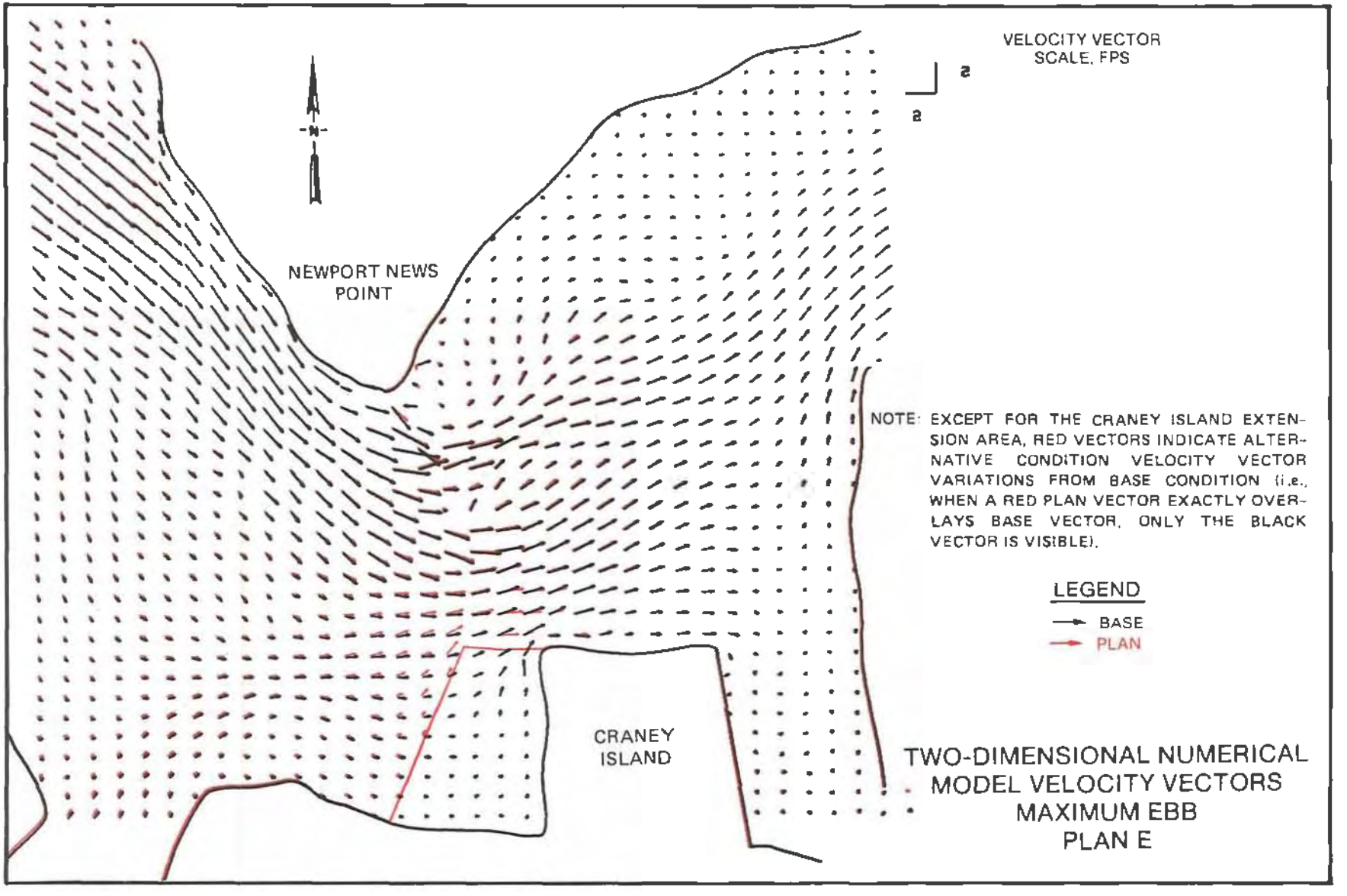
VELOCITY VECTOR
SCALE, FPS
2
2
NEWPORT NEWS
POINT
CRANEY
ISLAND
NOTE: EXCEPT FOR THE CRANEY ISLAND EXTENSION AREA, RED VECTORS INDICATE ALTERNATIVE CONDITION VELOCITY VECTOR VARIATIONS FROM BASE CONDITION (i.e., WHEN A RED PLAN VECTOR EXACTLY OVERLAYS BASE VECTOR, ONLY THE BLACK VECTOR IS VISIBLE).
LEGEND
BASE
PLAN
TWO-DIMENSIONAL NUMERICAL
MODEL VELOCITY VECTORS
MAXIMUM EBB
PLAN E

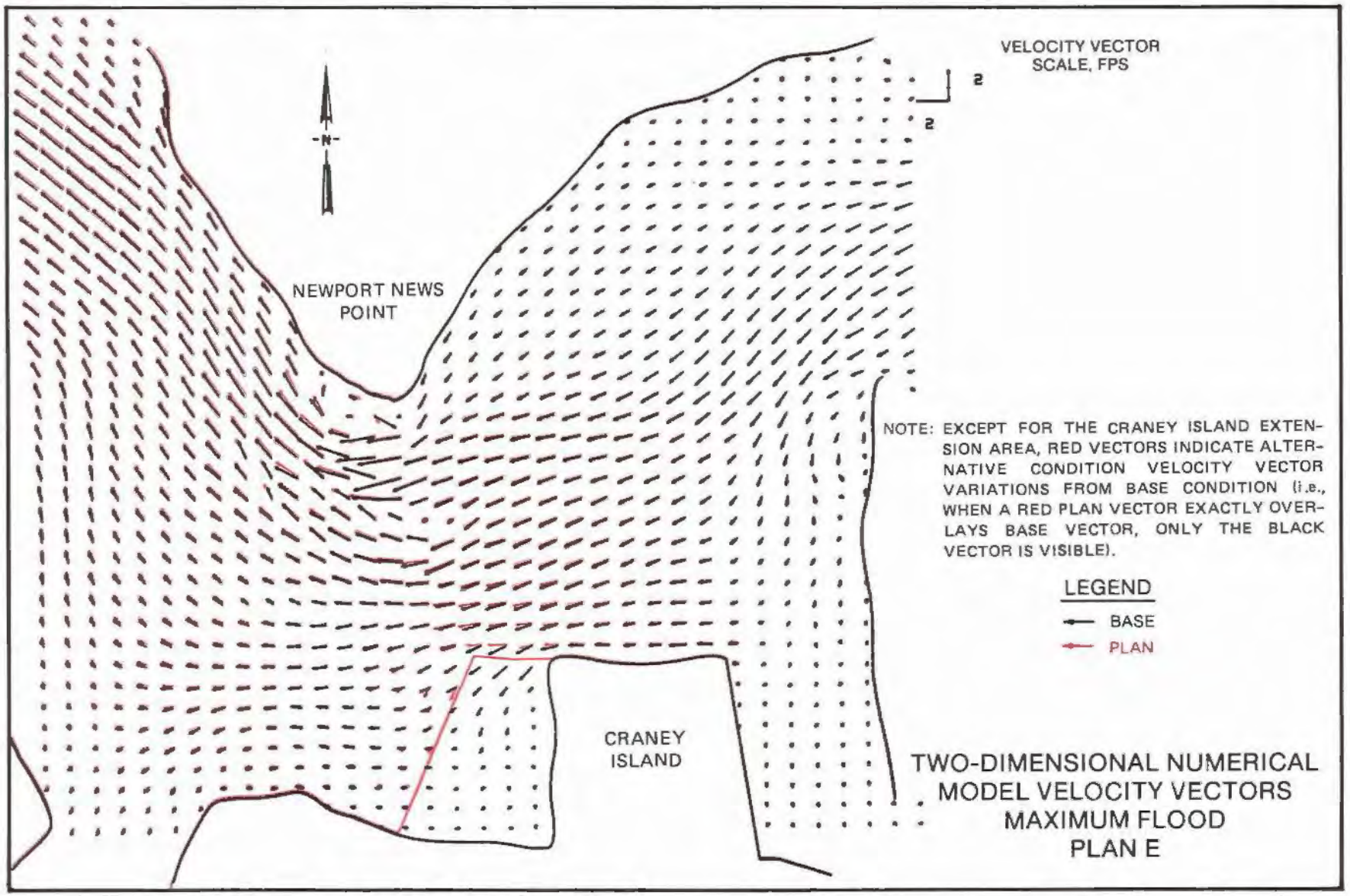
VELOCITY VECTOR
SCALE, FPS
2
2
N
NEWPORT NEWS
POINT
CRANEY
ISLAND
NOTE: EXCEPT FOR THE CRANEY ISLAND EXTENSION AREA, RED VECTORS INDICATE ALTERNATIVE CONDITION VELOCITY VECTOR VARIATIONS FROM BASE CONDITION (i.e., WHEN A RED PLAN VECTOR EXACTLY OVERLAYS BASE VECTOR, ONLY THE BLACK VECTOR IS VISIBLE).
LEGEND
BASE
PLAN
TWO-DIMENSIONAL NUMERICAL
MODEL VELOCITY VECTORS
MAXIMUM FLOOD
PLAN E

PLATE 10

PLATE 11

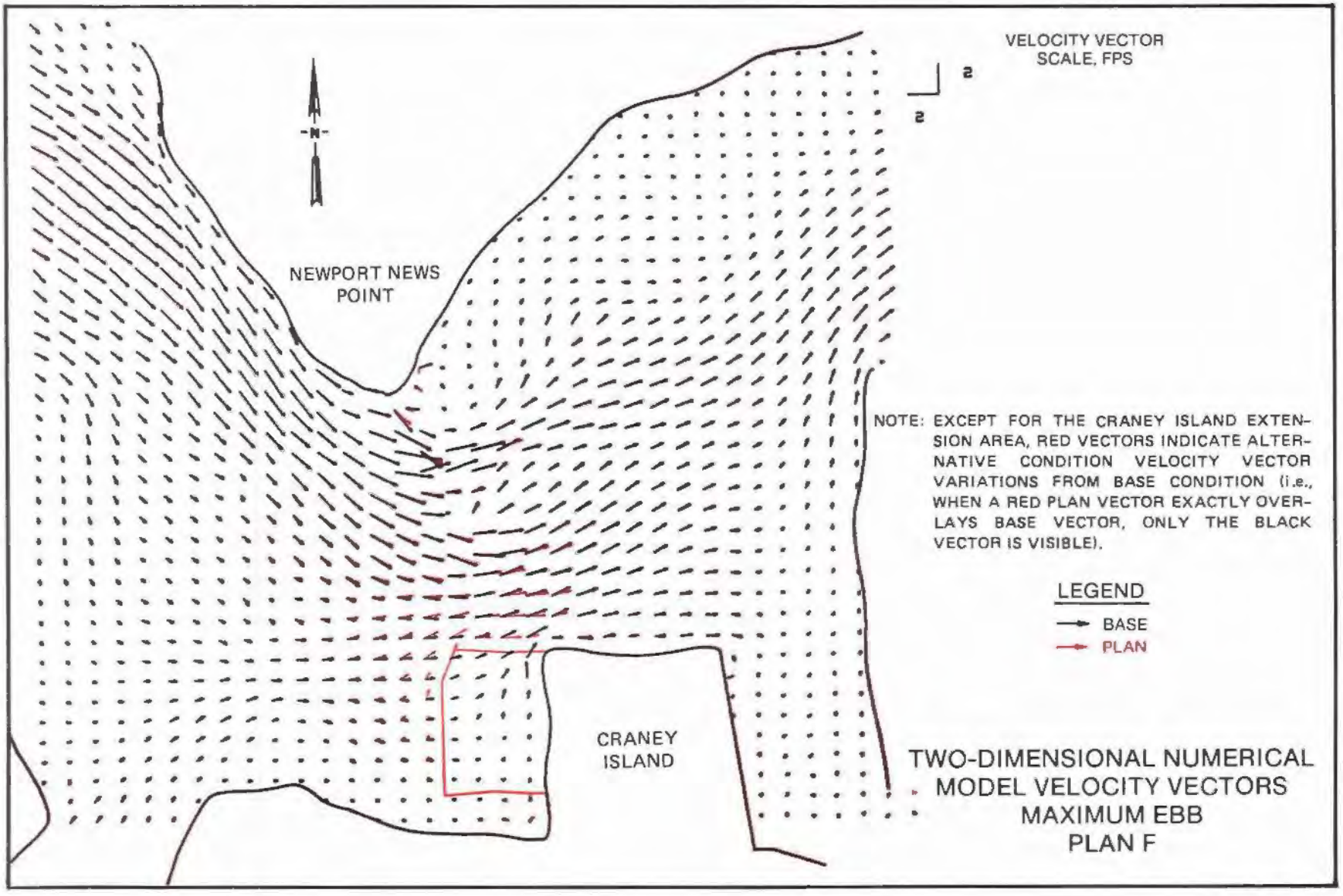
VELOCITY VECTOR
SCALE, FPS
2
2
N
NEWPORT NEWS
POINT
CRANEY
ISLAND
NOTE: EXCEPT FOR THE CRANEY ISLAND EXTENSION AREA, RED VECTORS INDICATE ALTERNATIVE CONDITION VELOCITY VECTOR VARIATIONS FROM BASE CONDITION (i.e., WHEN A RED PLAN VECTOR EXACTLY OVERLAYS BASE VECTOR, ONLY THE BLACK VECTOR IS VISIBLE).
LEGEND
BASE
PLAN
TWO-DIMENSIONAL NUMERICAL
MODEL VELOCITY VECTORS
MAXIMUM EBB
PLAN F

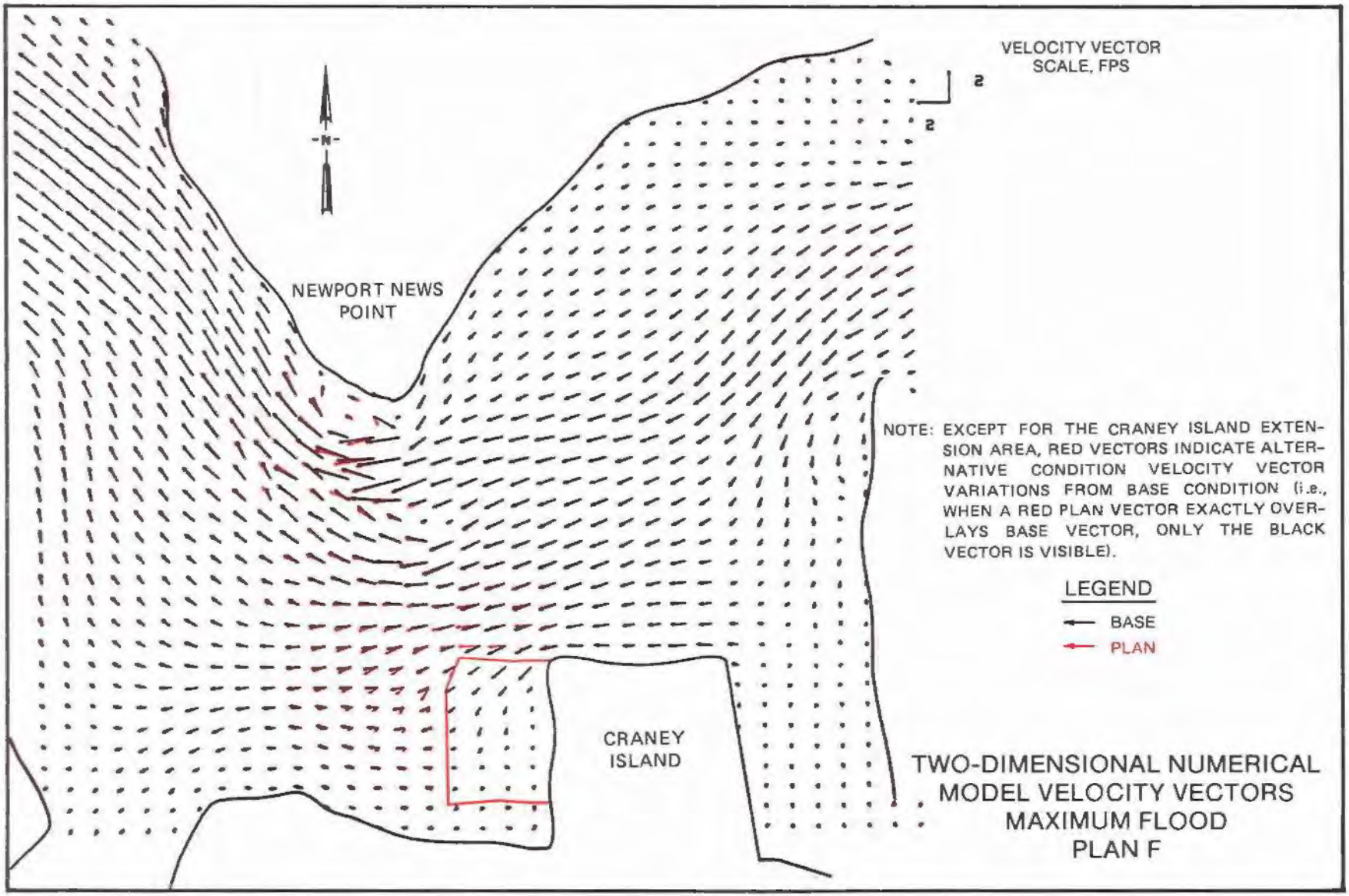
VELOCITY VECTOR
SCALE, FPS
2
2
N
NEWPORT NEWS
POINT
CRANEY
ISLAND
NOTE: EXCEPT FOR THE CRANEY ISLAND EXTENSION AREA, RED VECTORS INDICATE ALTERNATIVE CONDITION VELOCITY VECTOR VARIATIONS FROM BASE CONDITION (i.e., WHEN A RED PLAN VECTOR EXACTLY OVERLAYS BASE VECTOR, ONLY THE BLACK VECTOR IS VISIBLE).
LEGEND
BASE
PLAN
TWO-DIMENSIONAL NUMERICAL
MODEL VELOCITY VECTORS
MAXIMUM FLOOD
PLAN F

PLATE 12

PLATE 13

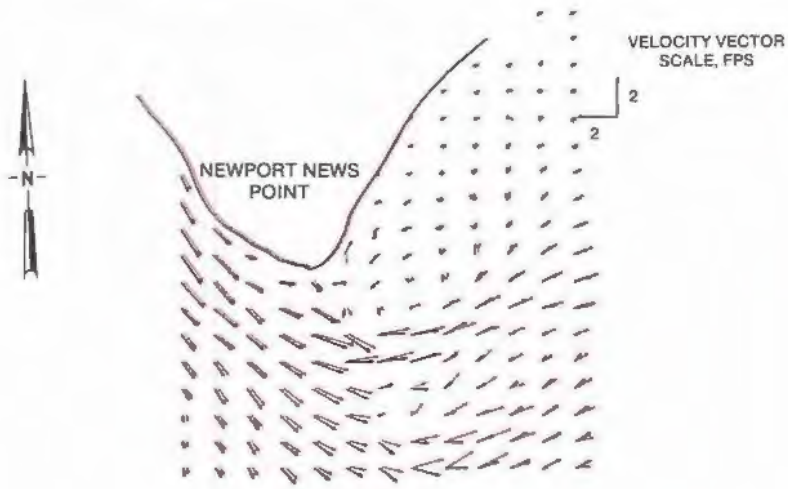

HOUR 15

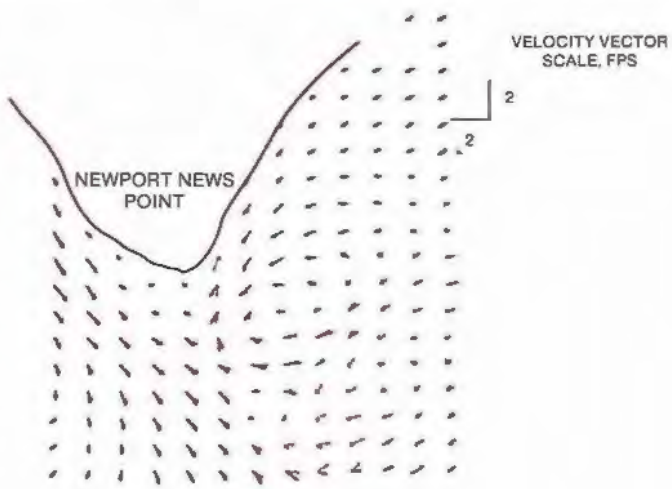

HOUR 16

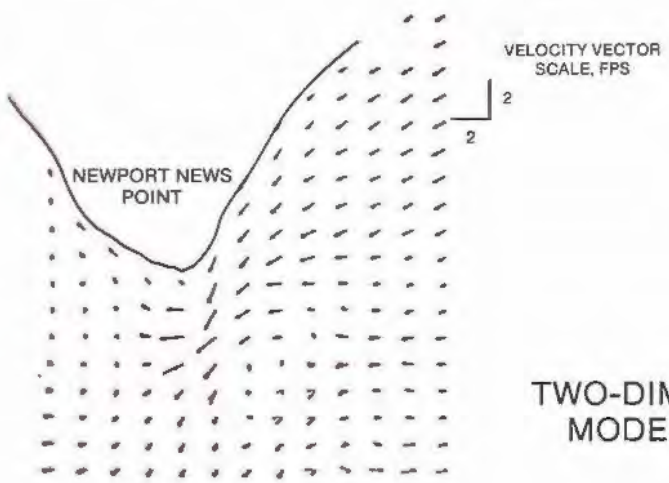

HOUR 17

LEGEND
BASE
PLAN

NOTE: RED VECTORS INDICATE ALTERNATIVE CONDITION VELOCITY VECTOR VARIATIONS FROM BASE CONDITION (i.e., WHEN A RED PLAN VECTOR EXACTLY OVERLAYS BASE VECTOR, ONLY THE BLACK VECTOR IS VISIBLE).

TWO-DIMENSIONAL NUMERICAL MODEL VELOCITY VECTORS HOURS 15-17 PLAN A

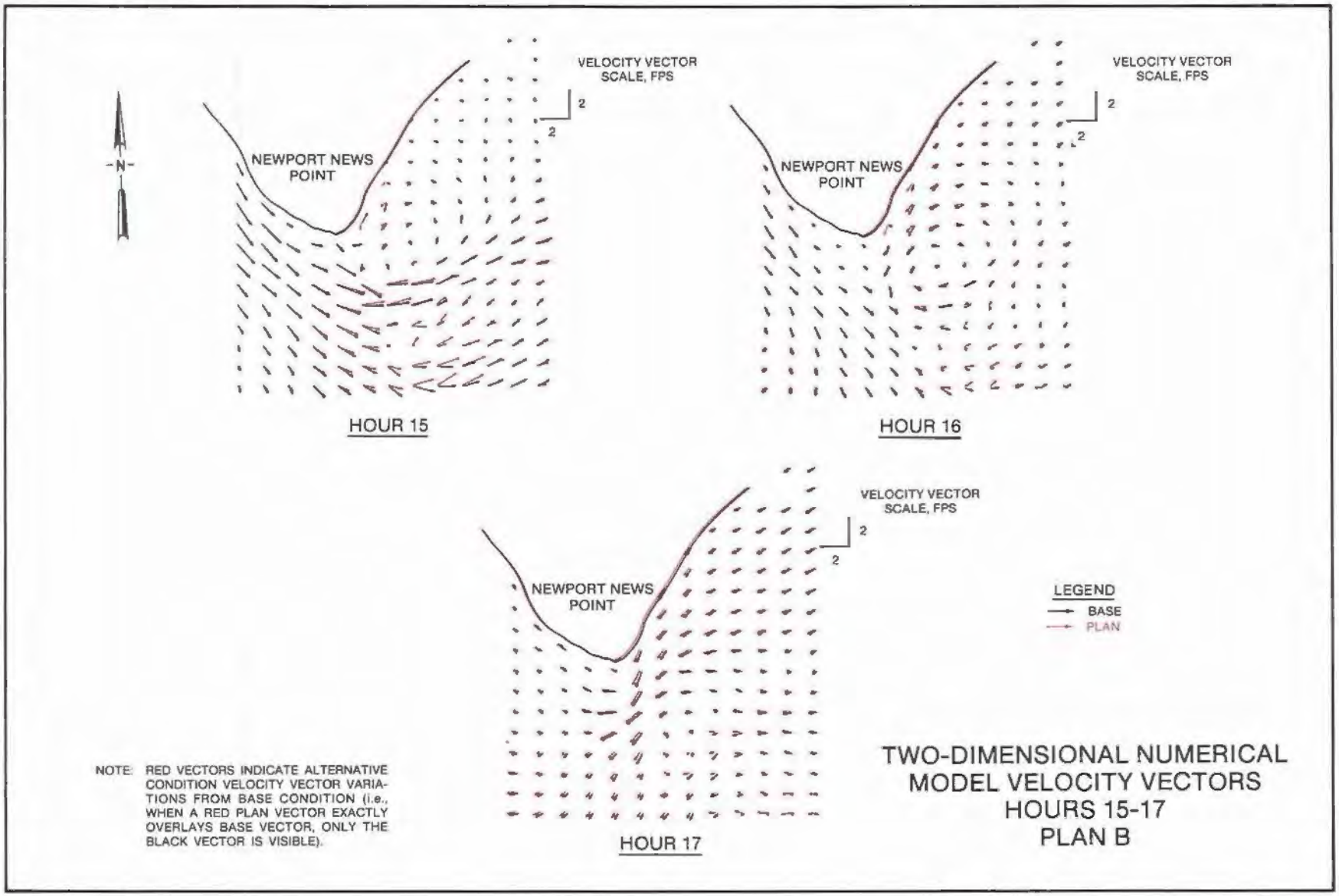

NOTE: RED VECTORS INDICATE ALTERNATIVE CONDITION VELOCITY VECTOR VARIATIONS FROM BASE CONDITION (i.e., WHEN A RED PLAN VECTOR EXACTLY OVERLAYS BASE VECTOR, ONLY THE BLACK VECTOR IS VISIBLE).

TWO-DIMENSIONAL NUMERICAL MODEL VELOCITY VECTORS HOURS 15-17 PLAN B

PLATE 14

PLATE 15

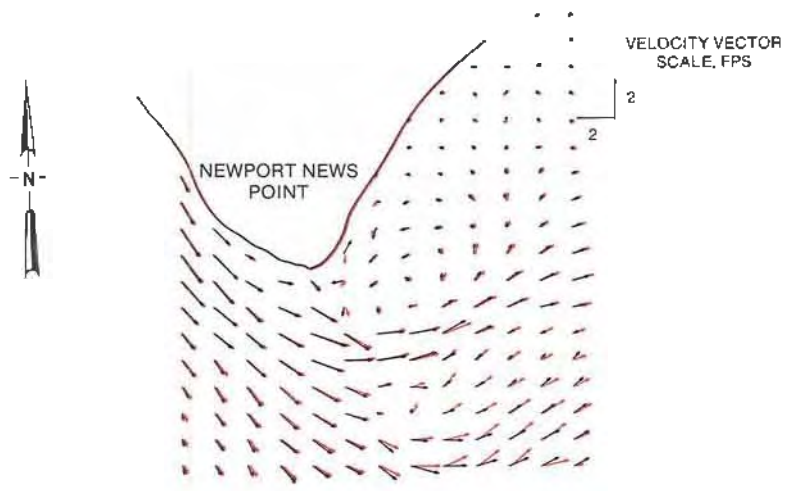

HOUR 15

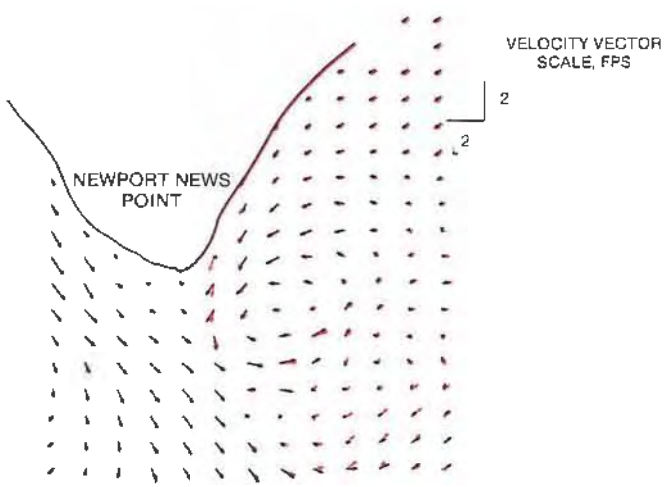

HOUR 16

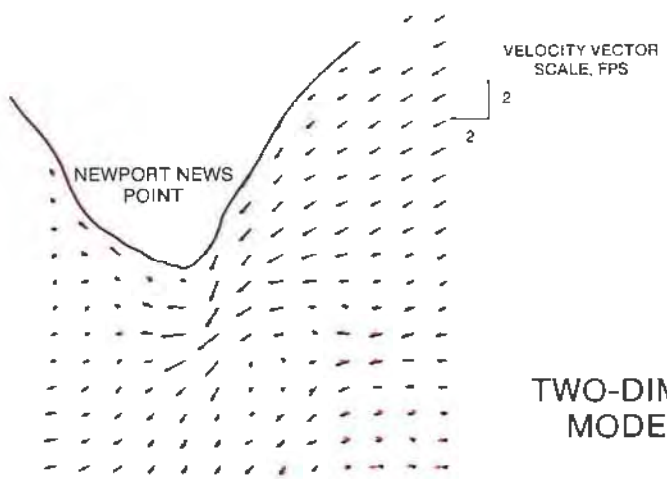

HOUR 17

LEGEND
BASE
PLAN

NOTE: RED VECTORS INDICATE ALTERNATIVE CONDITION VELOCITY VECTOR VARIATIONS FROM BASE CONDITION (i.e., WHEN A RED PLAN VECTOR EXACTLY OVERLAYS BASE VECTOR, ONLY THE BLACK VECTOR IS VISIBLE).

TWO-DIMENSIONAL NUMERICAL MODEL VELOCITY VECTORS HOURS 15-17 PLAN C

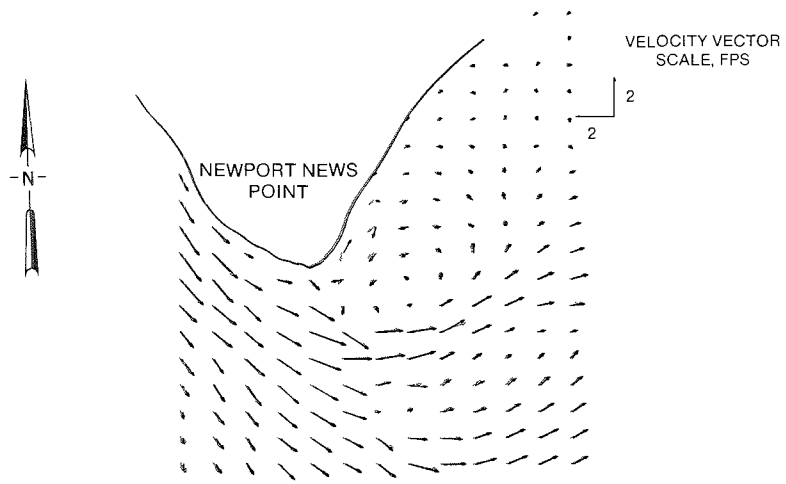

HOUR 15

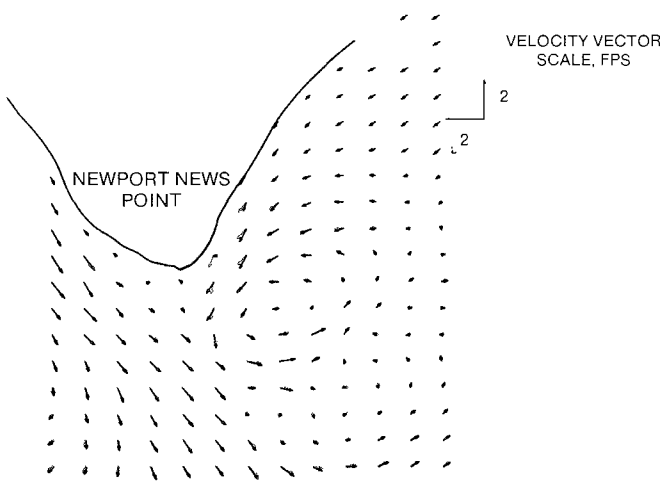

HOUR 16

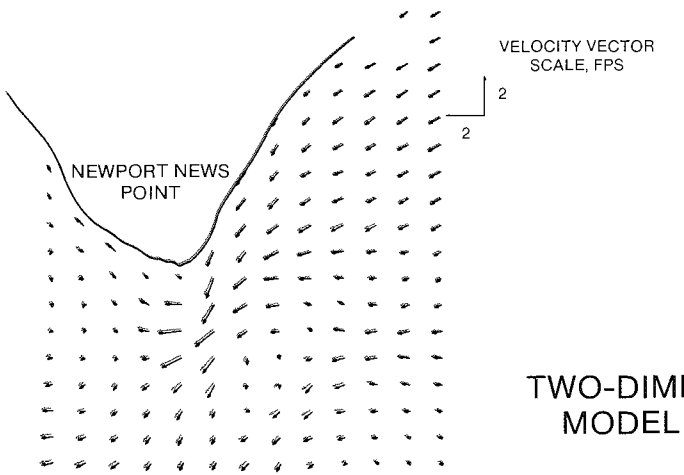

HOUR 17

LEGEND
BASE
PLAN

NOTE: RED VECTORS INDICATE ALTERNATIVE CONDITION VELOCITY VECTOR VARIATIONS FROM BASE CONDITION (i.e., WHEN A RED PLAN VECTOR EXACTLY OVERLAYS BASE VECTOR, ONLY THE BLACK VECTOR IS VISIBLE).

TWO-DIMENSIONAL NUMERICAL MODEL VELOCITY VECTORS HOURS 15-17 PLAN D

PLATE 16

PLATE 17

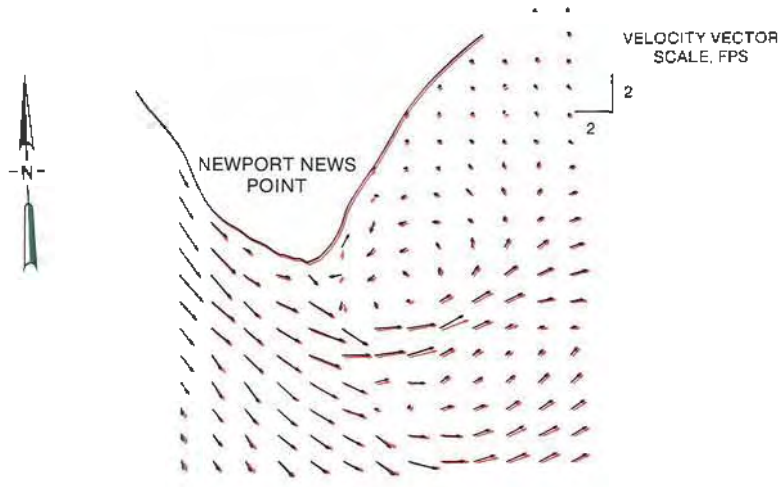

HOUR 15

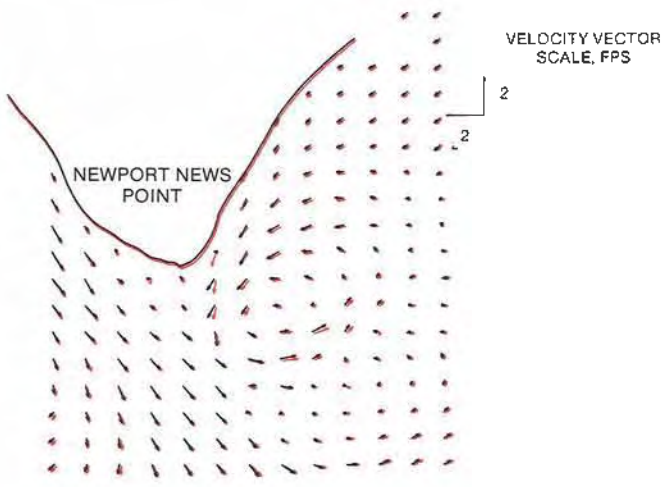

HOUR 16

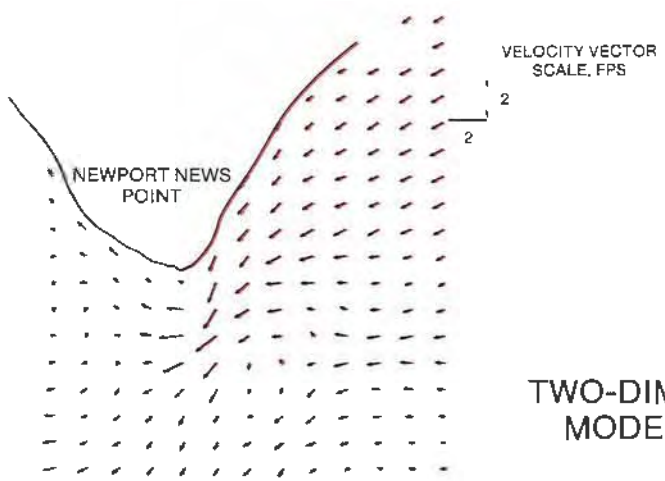

HOUR 17

LEGEND
BASE
PLAN

NOTE: RED VECTORS INDICATE ALTERNATIVE CONDITION VELOCITY VECTOR VARIATIONS FROM BASE CONDITION (i.e., WHEN A RED PLAN VECTOR EXACTLY OVERLAYS BASE VECTOR, ONLY THE BLACK VECTOR IS VISIBLE).

TWO-DIMENSIONAL NUMERICAL MODEL VELOCITY VECTORS HOURS 15-17 PLAN E

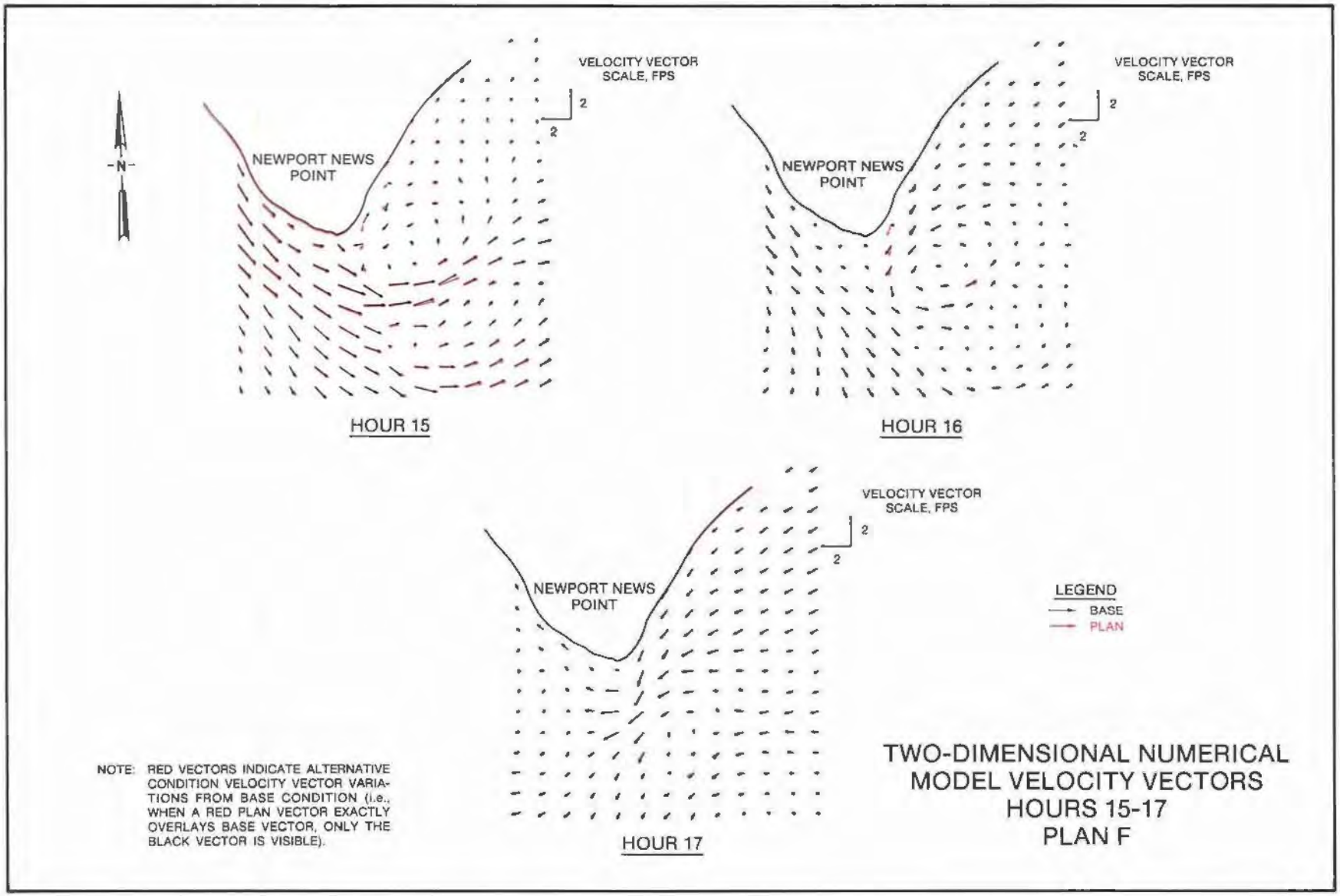
N
NEWPORT NEWS POINT
VELOCITY VECTOR SCALE, FPS
2
2
HOUR 15
NEWPORT NEWS POINT
VELOCITY VECTOR SCALE, FPS
2
2
HOUR 16
NEWPORT NEWS POINT
VELOCITY VECTOR SCALE, FPS
2
2
HOUR 17
LEGEND
BASE
PLAN
NOTE: RED VECTORS INDICATE ALTERNATIVE CONDITION VELOCITY VECTOR VARIATIONS FROM BASE CONDITION (i.e., WHEN A RED PLAN VECTOR EXACTLY OVERLAYS BASE VECTOR, ONLY THE BLACK VECTOR IS VISIBLE).
TWO-DIMENSIONAL NUMERICAL MODEL VELOCITY VECTORS
HOURS 15-17
PLAN F

PLATE 18

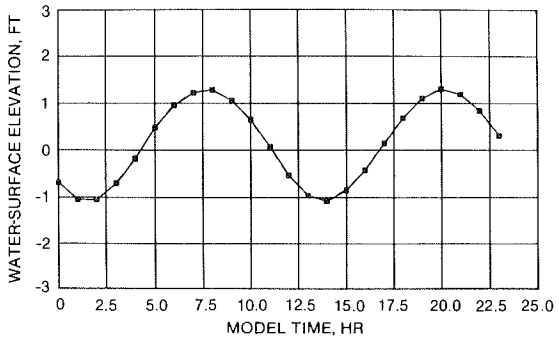

PLAN A

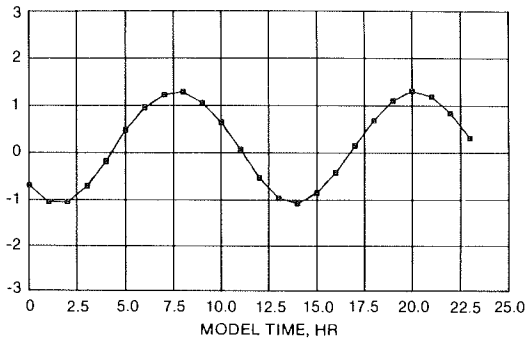

PLAN B

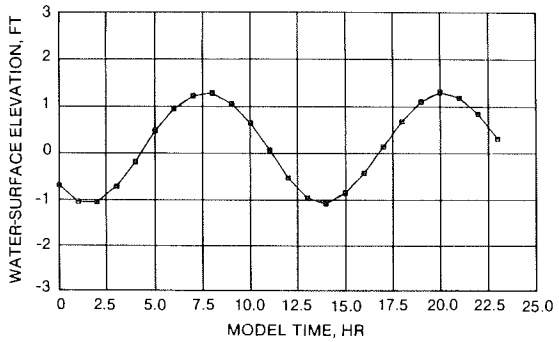

PLAN C

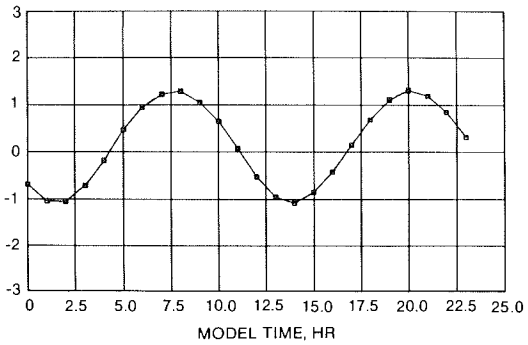

PLAN D

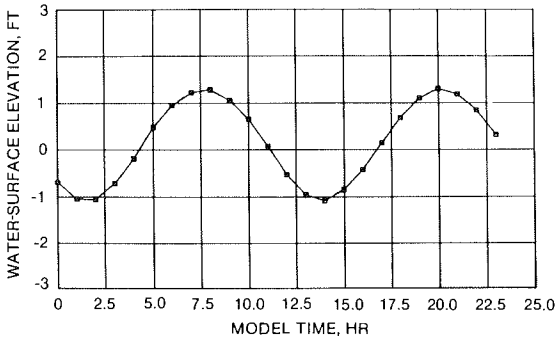

PLAN E

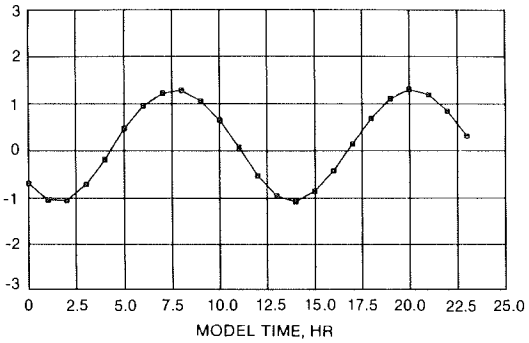

PLAN F

LEGEND

—— BASE

– – – PLAN

NOTE: SOLID CURVE INDICATES NO CHANGE

WATER-SURFACE TIME-HISTORIES BASE AND PLANS A-F NODE 18

PLATE 19

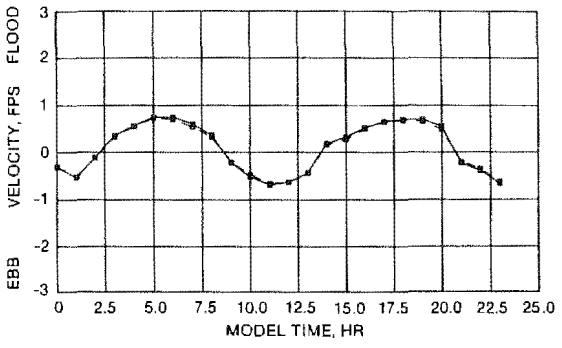

PLAN A

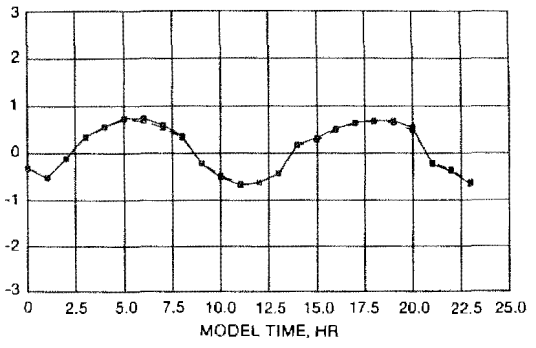

PLAN B

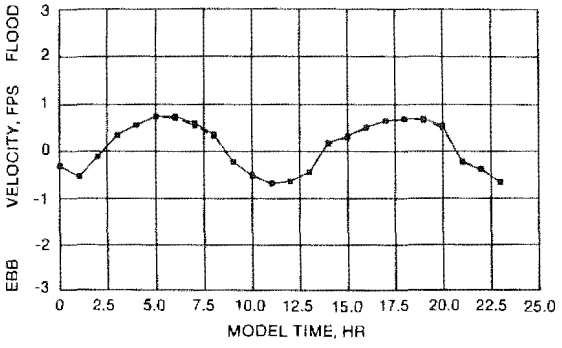

PLAN C

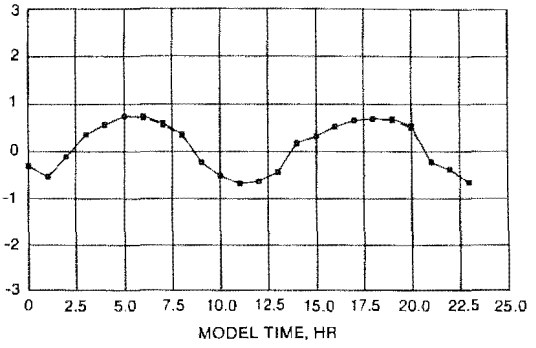

PLAN D

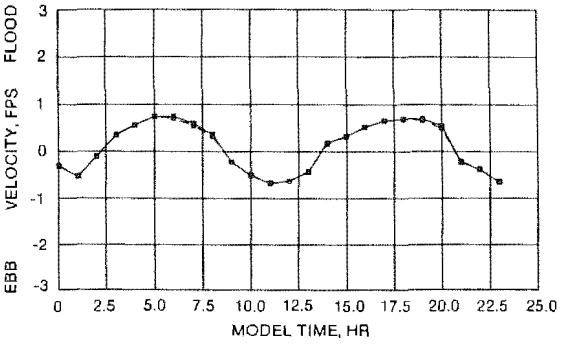

PLAN E

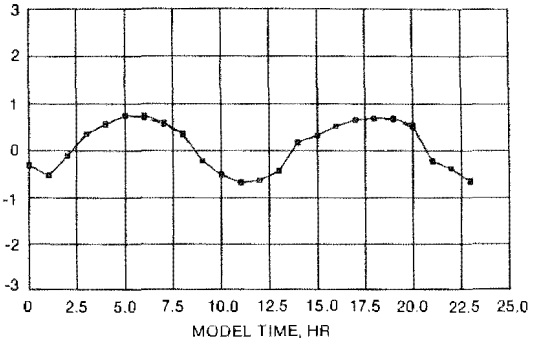

PLAN F

LEGEND

—— BASE

– – – PLAN

NOTE: SOLID CURVE INDICATES NO CHANGE

VELOCITY TIME-HISTORIES BASE AND PLANS A-F NODE 18

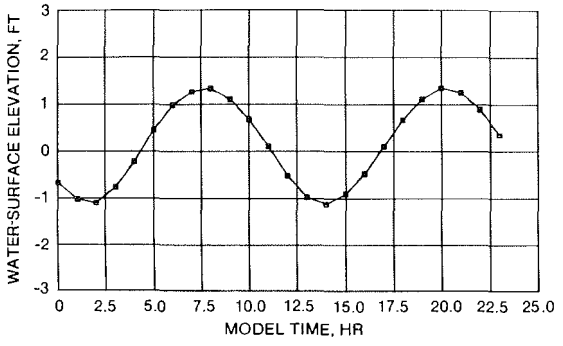

PLAN A

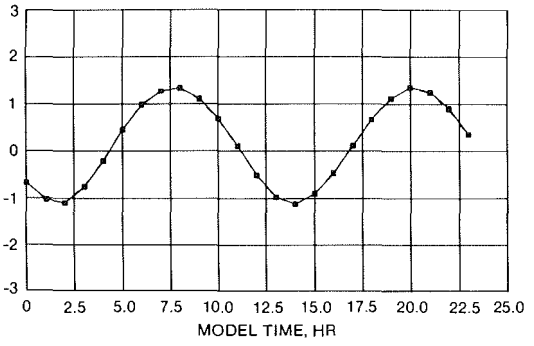

PLAN B

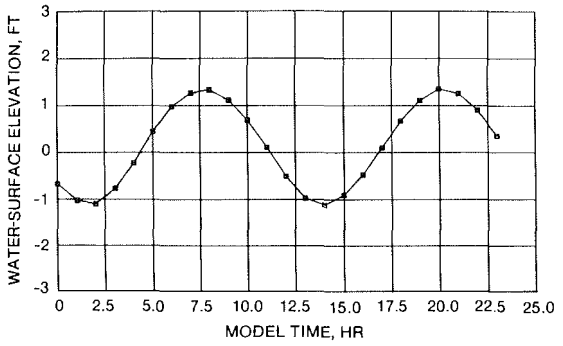

PLAN C

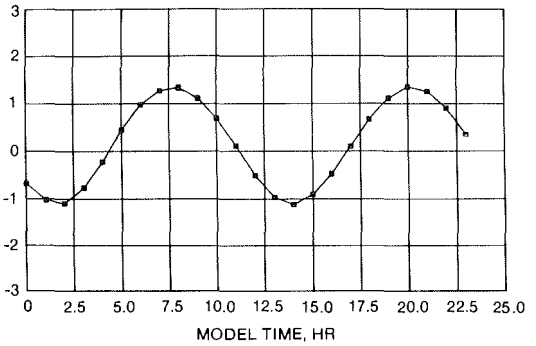

PLAN D

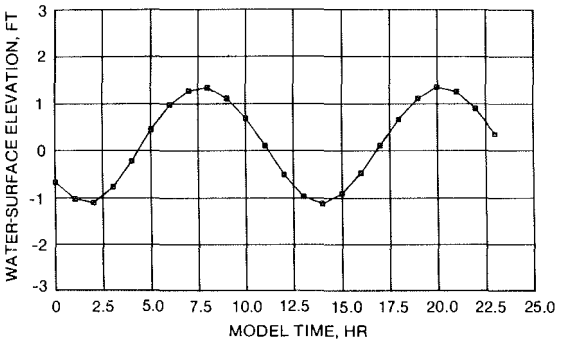

PLAN E

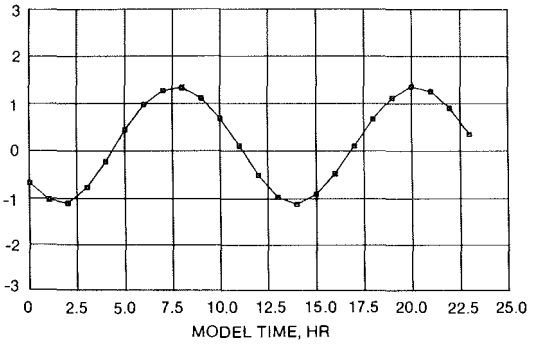

PLAN F

LEGEND

—— BASE

– – – PLAN

NOTE: SOLID CURVE INDICATES NO CHANGE

WATER-SURFACE TIME-HISTORIES BASE AND PLANS A-F NODE 146

PLATE 21

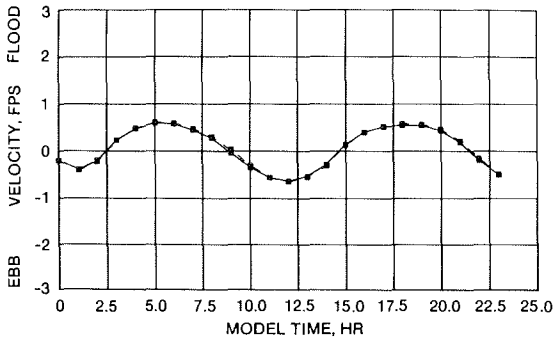

PLAN A

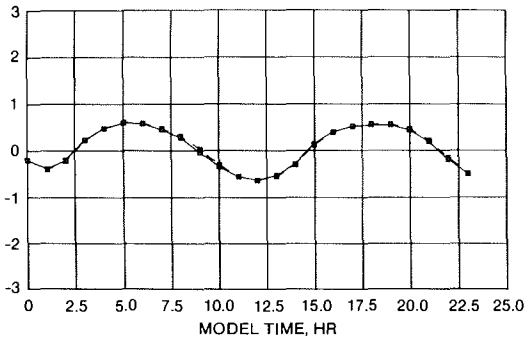

PLAN B

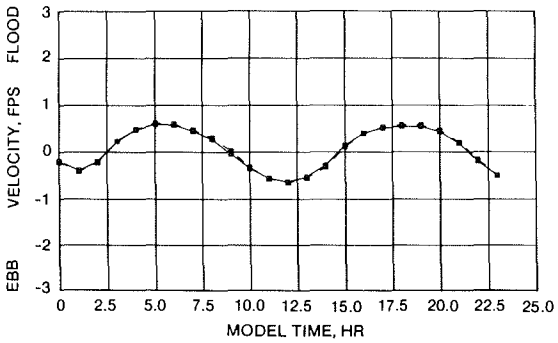

PLAN C

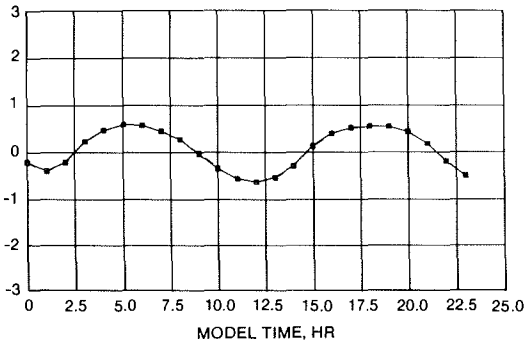

PLAN D

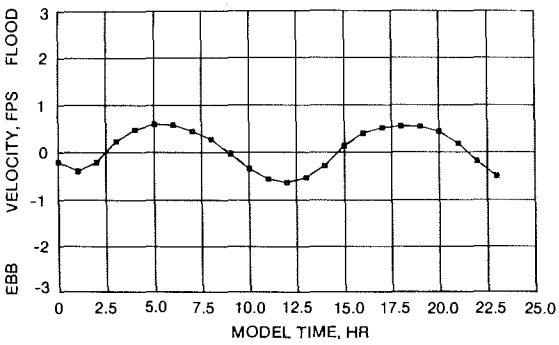

PLAN E

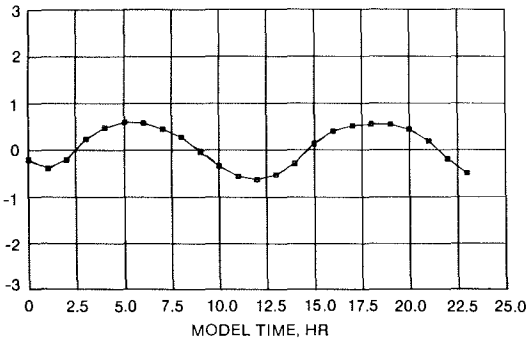

PLAN F

LEGEND

—— BASE

– – – PLAN

NOTE: SOLID CURVE INDICATES NO CHANGE

VELOCITY TIME-HISTORIES BASE AND PLANS A-F NODE 146

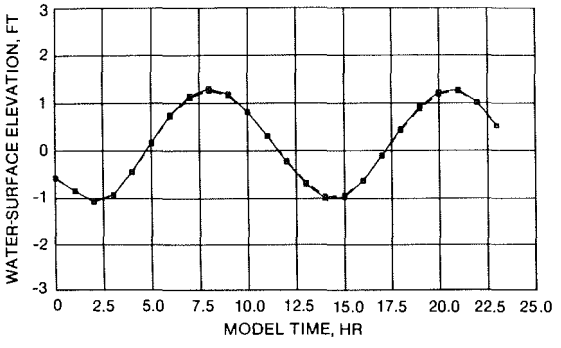

PLAN A

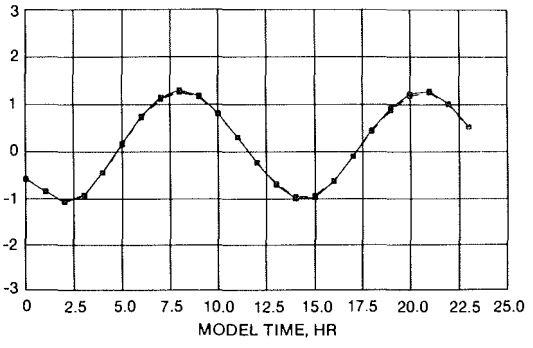

PLAN B

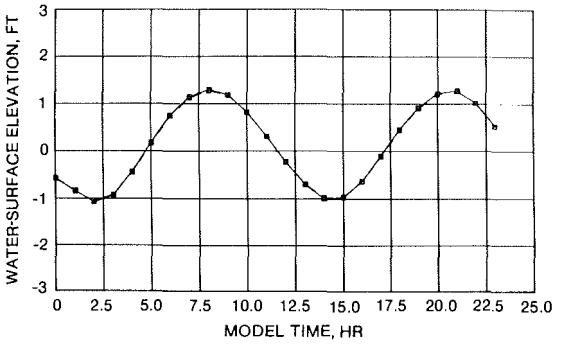

PLAN C

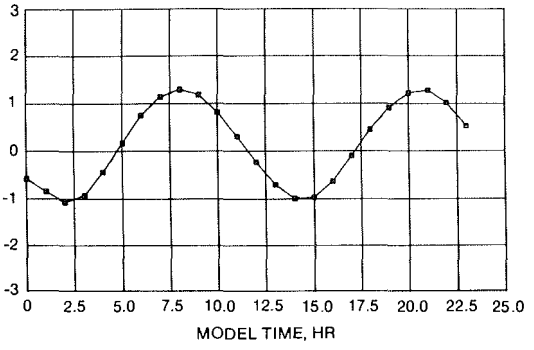

PLAN D

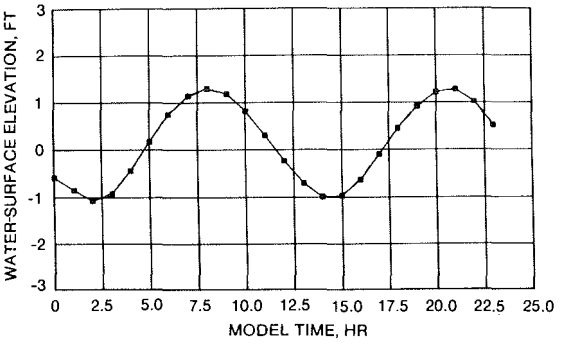

PLAN E

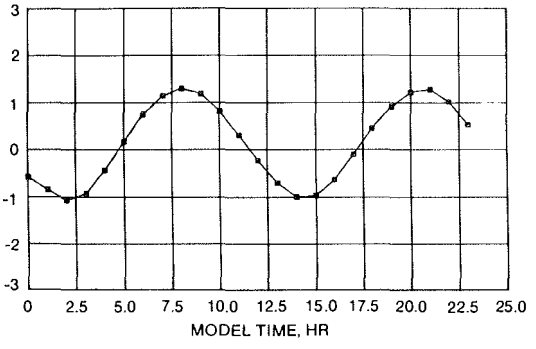

PLAN F

LEGEND
—— BASE
--- PLAN

NOTE: SOLID CURVE INDICATES NO CHANGE

WATER-SURFACE TIME-HISTORIES
BASE AND PLANS A-F
NODE 677

PLATE 23

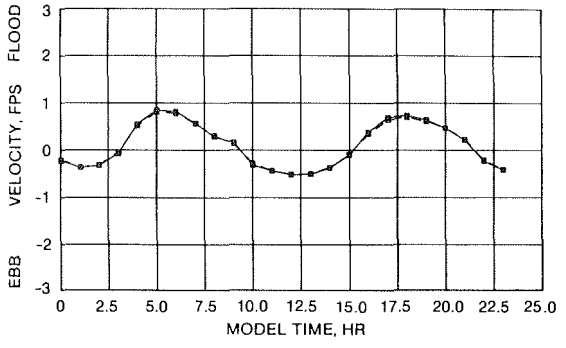

PLAN A

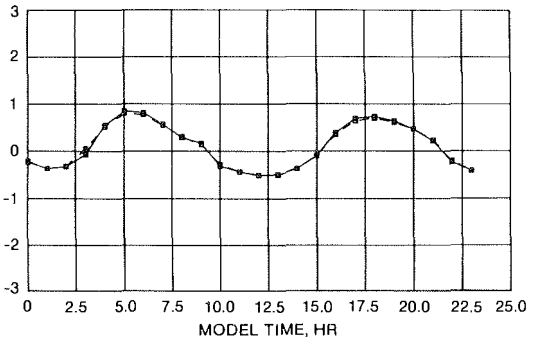

PLAN B

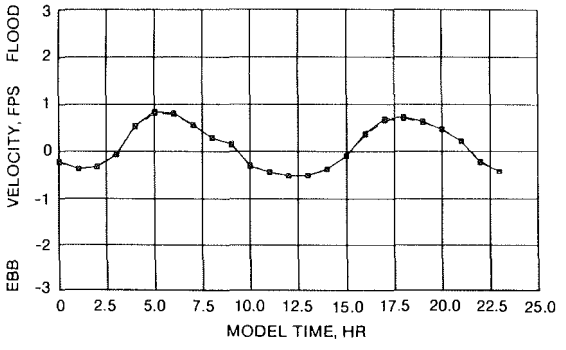

PLAN C

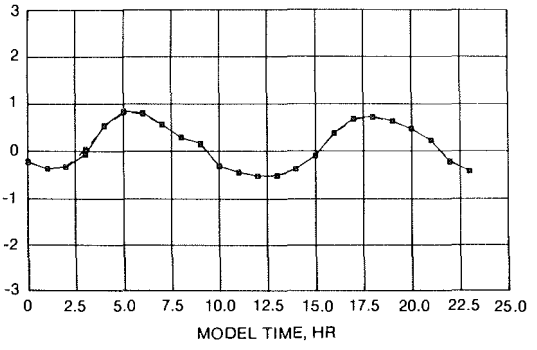

PLAN D

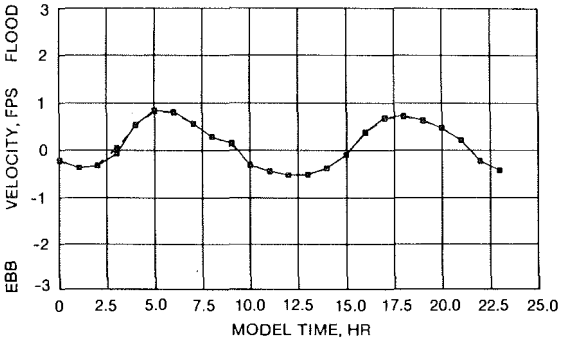

PLAN E

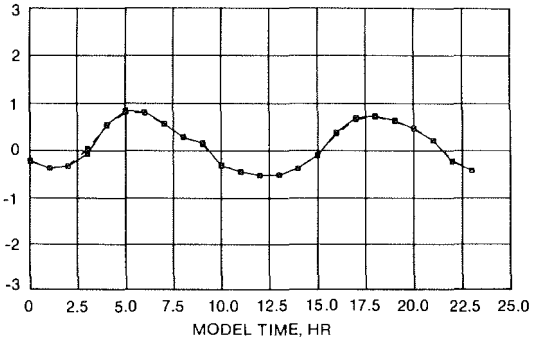

PLAN F

LEGEND

—— BASE

– – – PLAN

NOTE: SOLID CURVE INDICATES NO CHANGE

VELOCITY TIME-HISTORIES BASE AND PLANS A-F NODE 677

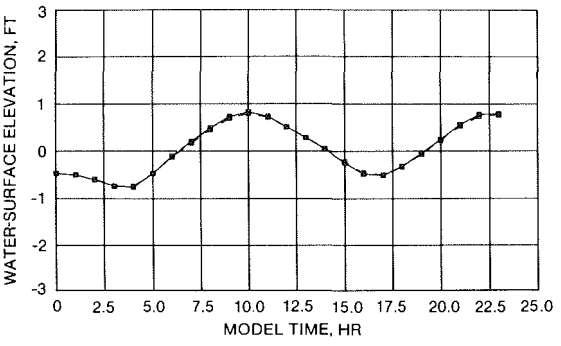

PLAN A

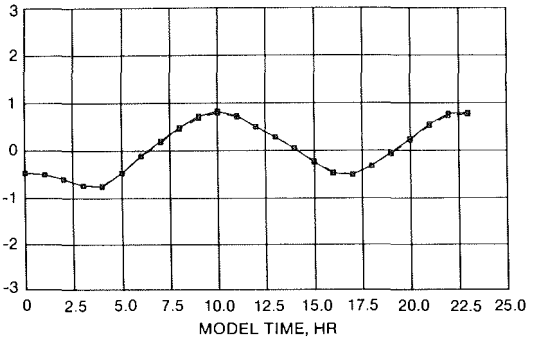

PLAN B

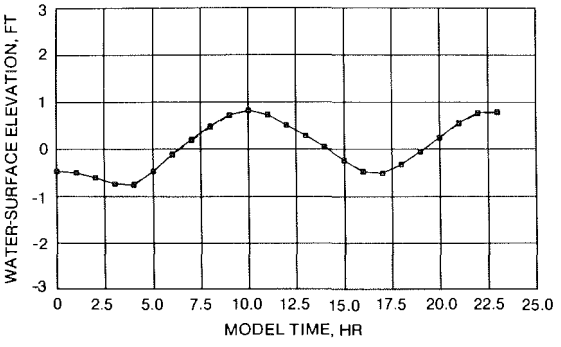

PLAN C

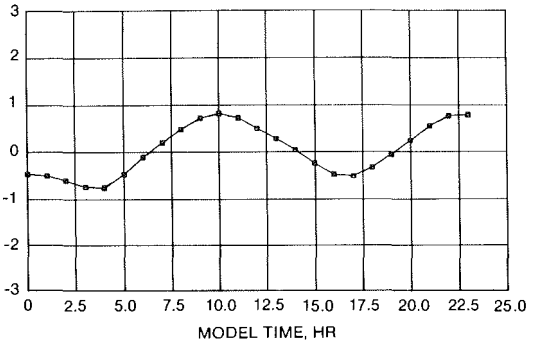

PLAN D

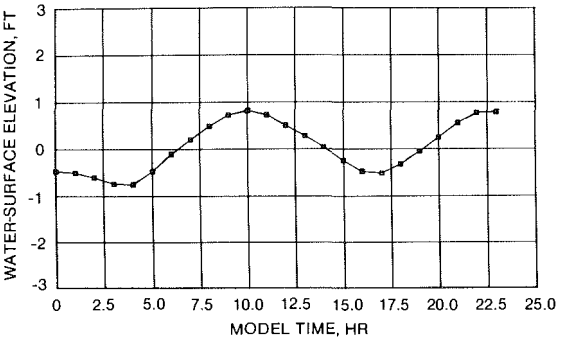

PLAN E

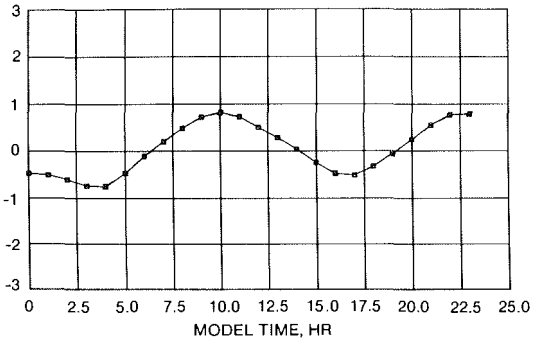

PLAN F

LEGEND

—— BASE

– – – PLAN

NOTE: SOLID CURVE INDICATES NO CHANGE

WATER-SURFACE TIME-HISTORIES BASE AND PLANS A-F NODE 1258

PLATE 25

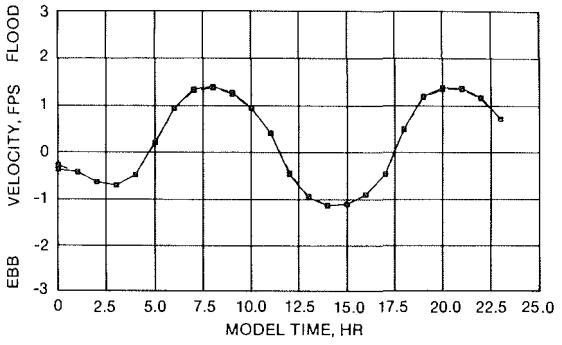

PLAN A

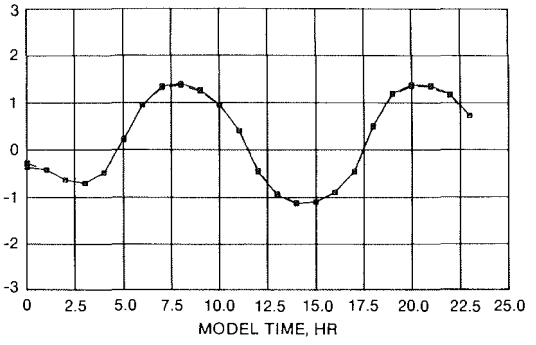

PLAN B

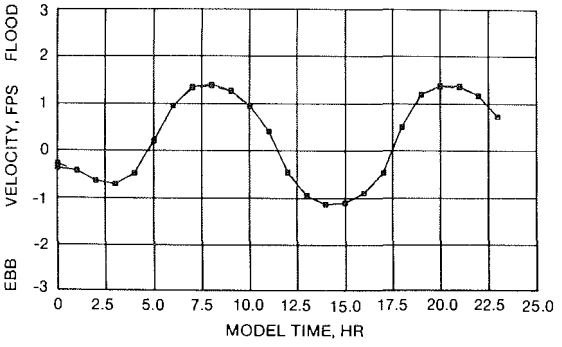

PLAN C

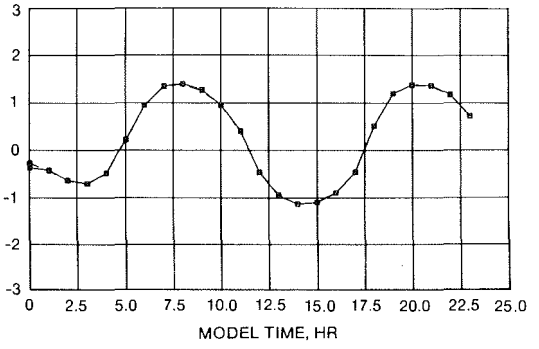

PLAN D

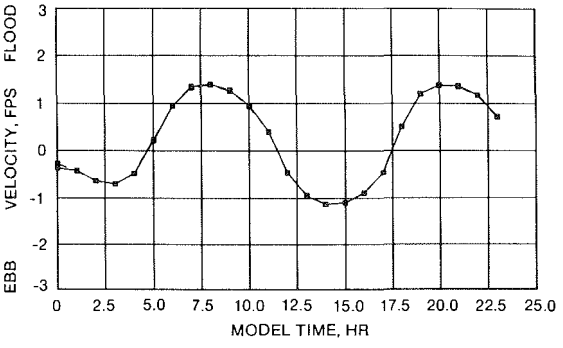

PLAN E

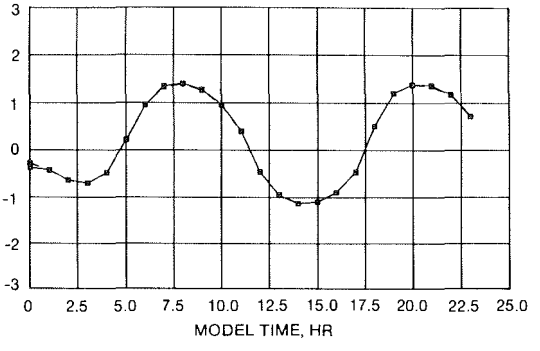

PLAN F

LEGEND

—— BASE

– – – PLAN

NOTE: SOLID CURVE INDICATES NO CHANGE

VELOCITY TIME-HISTORIES BASE AND PLANS A-F NODE 1258

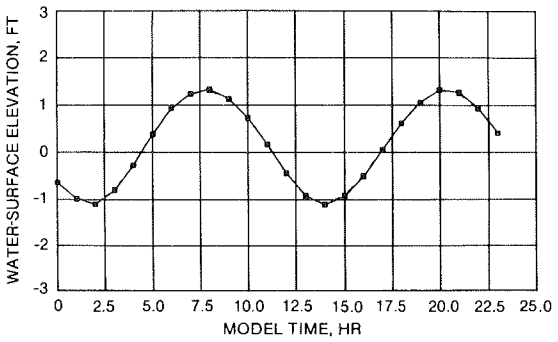

PLAN A

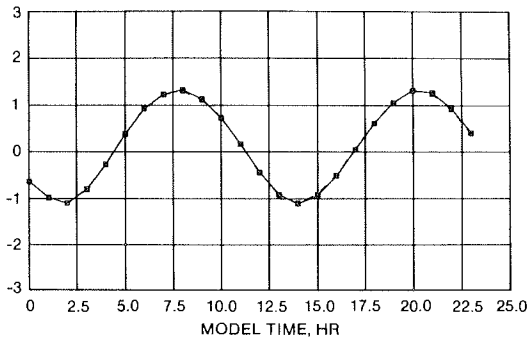

PLAN B

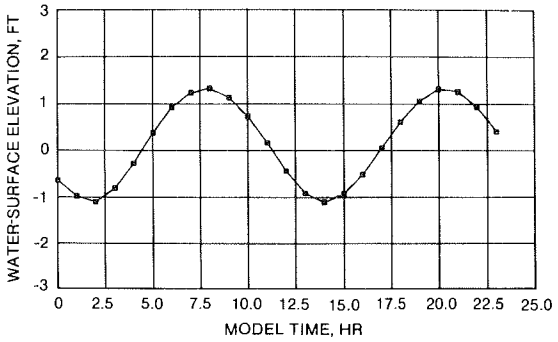

PLAN C

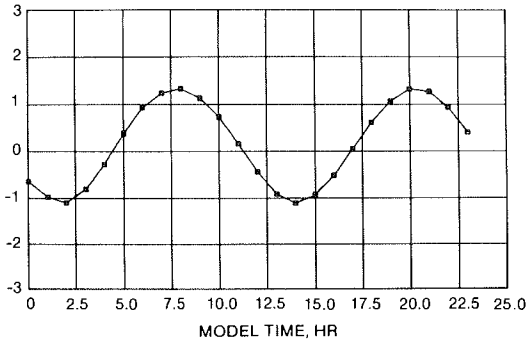

PLAN D

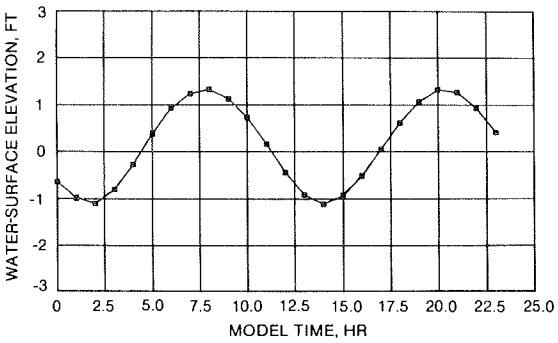

PLAN E

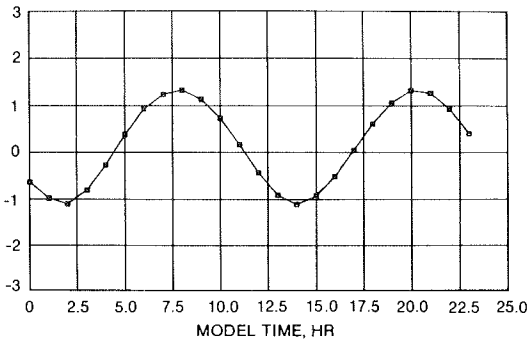

PLAN F

LEGEND

—— BASE

– – – PLAN

NOTE: SOLID CURVE INDICATES NO CHANGE

WATER-SURFACE TIME-HISTORIES BASE AND PLANS A-F NODE 1980

PLATE 27

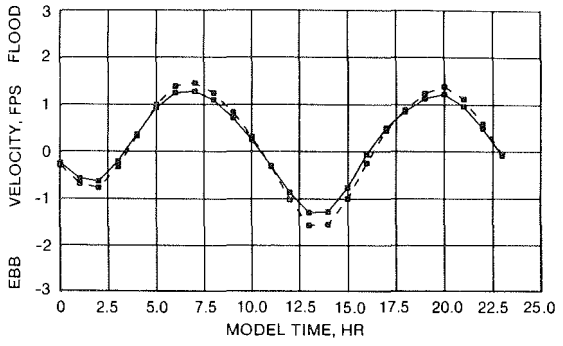

PLAN A

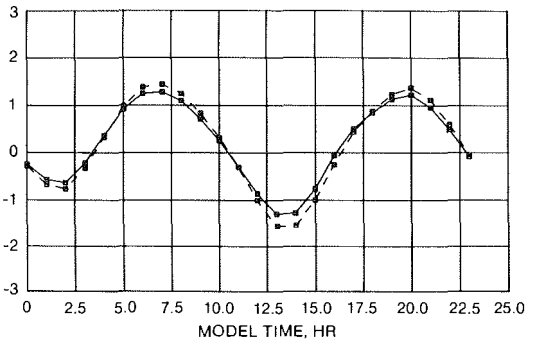

PLAN B

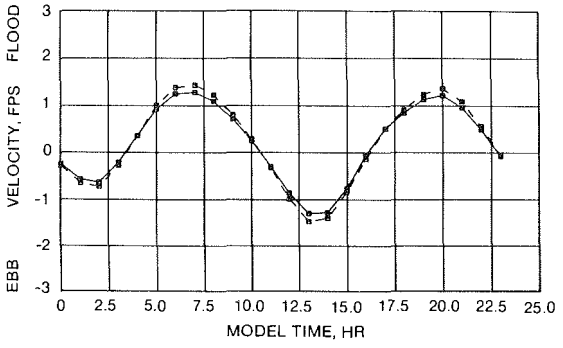

PLAN C

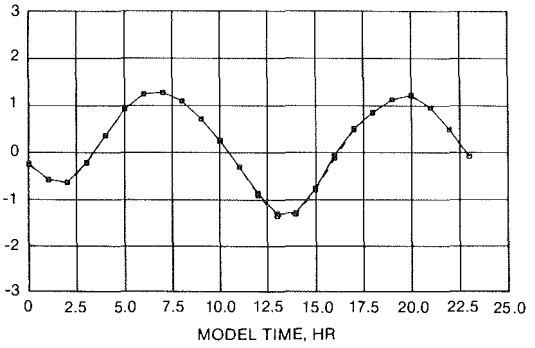

PLAN D

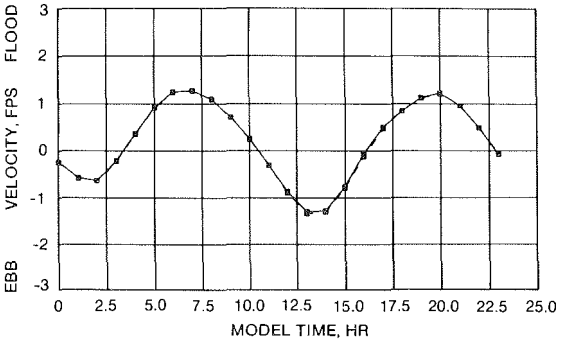

PLAN E

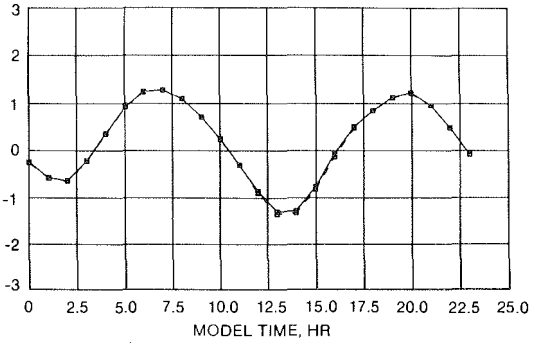

PLAN F

LEGEND

—— BASE

– – – PLAN

NOTE: SOLID CURVE INDICATES NO CHANGE

VELOCITY TIME-HISTORIES BASE AND PLANS A-F NODE 1980

PLATE 28

APPENDIX A: FINITE ELEMENT MODELING*

1. The TABS-2 numerical models used in this effort employ the finite element method to solve the governing equations. To help those who are unfamiliar with the method to better understand this report, a brief description of the method is given here. For a more thorough treatment, see Zienkiewicz (1971)** or Desai (1979).

2. The finite element method approximates a solution to equations by dividing the area of interest into smaller subareas, which are called elements. The dependent variables (e.g., water-surface elevations and sediment concentrations) are approximated over each element by continuous functions which interpolate in terms of unknown point (node) values of the variables. An error, defined as the deviation of the approximation solution from the correct solution, is minimized. Then, when boundary conditions are imposed, a set of solvable simultaneous equations is created. The solution is smooth and continuous over the area of interest.

3. In one-dimensional problems, elements are line segments. In two-dimensional problems, the elements are polygons, usually either triangles or quadrilaterals. Nodes are located on the edges of elements and occasionally inside the elements. The interpolating functions may be linear or higher order polynomials. Figure A1 illustrates a quadrilateral element with eight nodes and a linear solution surface.

4. Most water resource applications of the finite element method use the Galerkin method of weighted residuals to minimize error. In this method the residual, the total error between the approximate and correct solutions, is weighted by a function that is identical with the interpolating function and then minimized. Minimization results in a set of simultaneous equations in terms of nodal values of the dependent variable (e.g., water-surface elevations or sediment concentration). Time-dependent problems can have the time portion solved by the finite element methods, but it is generally more efficient to express derivatives with respect to time in finite difference form.

5. The finite difference method, sometimes called FDM, is another technique used in numerical modeling. The FDM solves mathematical models by

---

* Paragraphs 1-4 of this appendix from Stewart, Daggett, and Athow (1985).
** All references cited in this appendix are listed in the References at the end of the main text.

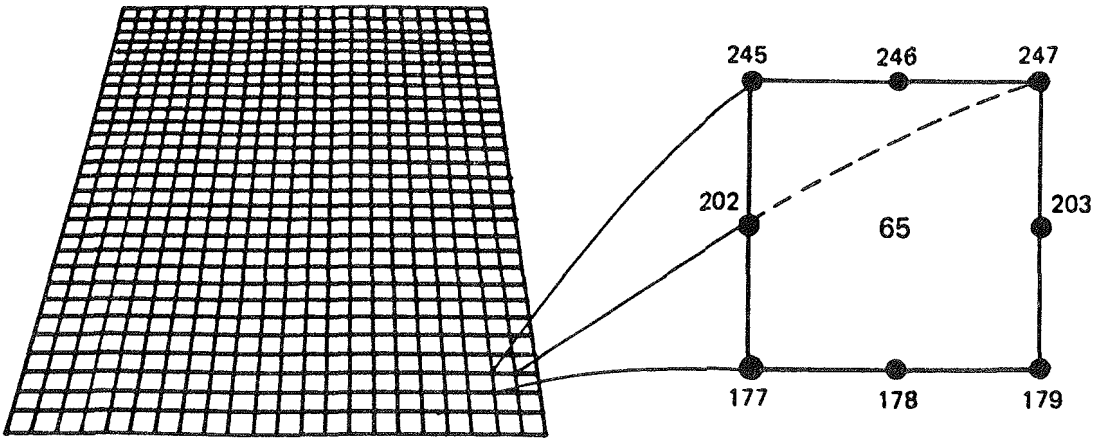

a. Eight nodes define each element

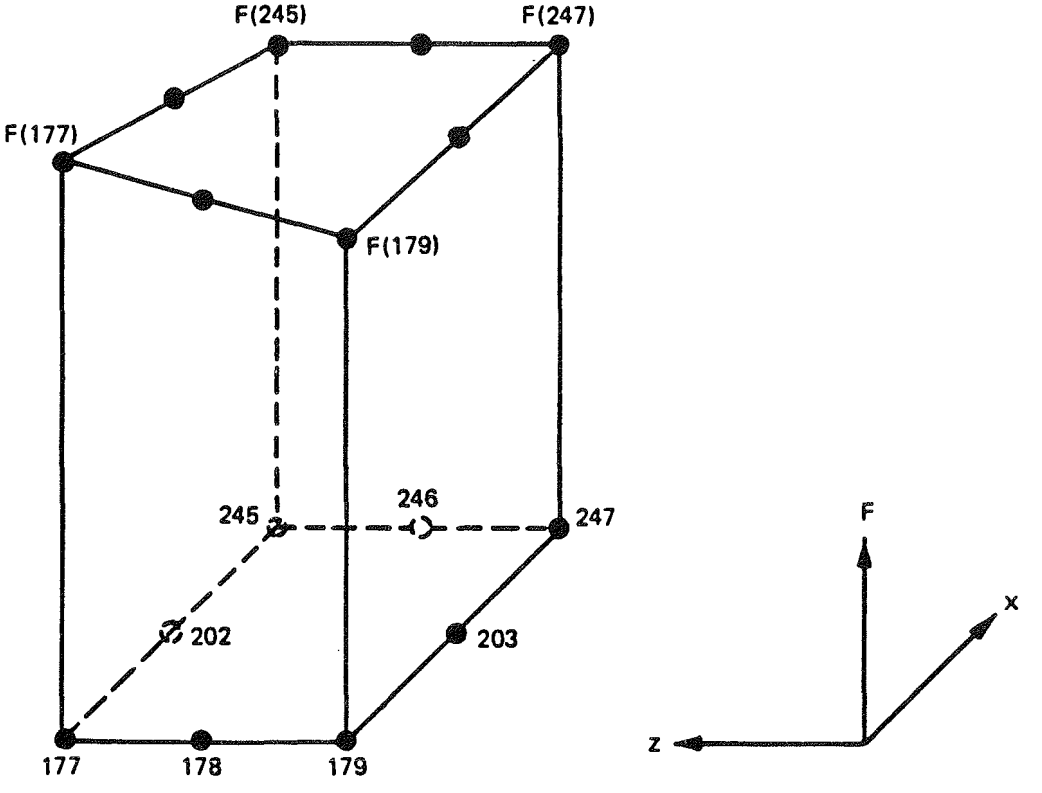

b. Linear interpolation function

Figure A1. Two-dimensional finite element mesh

approximating derivatives with differences in the value of variables over finite intervals of space and time. It requires discretization of space and time into more or less regular grids of computational points. The finite difference method obtains solutions to approximate equations.

6. In summary, the finite element method, sometimes called FEM, provides a means of obtaining an approximate solution to a system of governing equations; the partial differential equations are transformed into finite element form and then solved in a global matrix system. The solution is smooth over each element and continuous over the computational network, and the spatial integral of the error is minimized. In comparison, conventional finite difference methods provide a means of obtaining a solution to approximate equations of the governing equations; the partial differential equation terms are usually replaced by difference quotients and solved at discrete points.

7. Simply stated, conventional finite difference methods approximate the equations to be solved, then provide solutions to the approximate equations giving approximate answers for discrete points. Finite element methods approximate the form of the solution and then solve the governing equations providing a continuous approximate solution over the modeled area of interest. Both finite difference and finite element methods provide approximate solutions to the same basic equations for conservation of mass and momentum.

APPENDIX B: THE HYDRODYNAMIC MODEL, RMA-2V*

1. The generalized computer program RMA-2 solves the depth-integrated equations of fluid mass and momentum conservation in two horizontal directions. The form of the solved equations is

$$\frac{\partial u}{\partial t} + u\frac{\partial u}{\partial x} + w\frac{\partial u}{\partial z} + g\left(\frac{\partial h}{\partial x} + \frac{\partial a_o}{\partial x}\right) - \frac{\varepsilon_{xx}}{\rho}\frac{\partial^2 u}{\partial x^2} - \frac{\varepsilon_{xz}}{\rho}\frac{\partial^2 u}{\partial z^2}$$

$$-2\omega w \sin\phi + \frac{gu}{C^2 h}\left(u^2 + w^2\right)^{1/2} - \frac{\xi}{h}V_a^2 \cos\Psi = 0 \qquad \text{(B1)}$$

$$\frac{\partial w}{\partial t} + u\frac{\partial w}{\partial x} + w\frac{\partial w}{\partial z} + g\left(\frac{\partial h}{\partial z} + \frac{\partial a_o}{\partial z}\right) - \frac{\varepsilon_{zx}}{\rho}\frac{\partial^2 w}{\partial x^2} - \frac{\varepsilon_{zz}}{\rho}\frac{\partial^2 w}{\partial z^2} + 2\omega u \sin\phi$$

$$+ \frac{gw}{C^2 h}\left(u^2 + w^2\right)^{1/2} - \frac{\xi}{h}V_a^2 \sin\Psi = 0 \qquad \text{(B2)}$$

$$\frac{\partial h}{\partial t} + \frac{\partial}{\partial x}(uh) + \frac{\partial}{\partial z}(wh) = 0 \qquad \text{(B3)}$$

where

u = horizontal flow velocity in the x-direction
t = time
x = distance in the x-direction (longitudinal)
w = horizontal flow velocity in the z-direction
z = distance in the z-direction (lateral)
g = acceleration due to gravity
h = water depth
a_o = elevation of the bottom
ε_{xx} = normal turbulent exchange coefficient in the x-direction
ρ = fluid density
ε_{xz} = tangential turbulent exchange coefficient in the x-direction

---

* This appendix from Stewart, Daggett, and Athow (1985).

ω = angular rate of earth's rotation

ϕ = latitude

C = Chezy roughness coefficient

ξ = coefficient relating wind speed to stress exerted on the fluid

V_a = wind velocity

Ψ = angle between wind direction and x-axis

ε_{zx} = tangential turbulent exchange coefficient in the z-direction

ε_{zz} = normal turbulent exchange coefficient in the z-direction

2. The Chezy roughness formulation of the original code was modified in the input portion so that Manning's n roughness coefficients may be specified from input Manning's n values and initial water depth.

3. Equations B1, B2, and B3 are solved by the finite element method using Galerkin weighted residuals. The elements may be either quadrilaterals or triangles and may have curved (parabolic) sides. The shape functions are quadratic for flow and linear for depth. Integration in space is performed by Gaussian integration. Derivatives in time are replaced by a nonlinear finite difference approximation. Variables are assumed to vary over each time interval in the form

$$f(t) = f(0) + at + bt^c \qquad t_o \leq t < t_1 \tag{B4}$$

which is differentiated with respect to time, and cast in finite difference form. Letters a , b , and c are constants. It has been found by experiment that the best value for c is 1.5 (Norton and King 1977).*

4. The solution is fully implicit and the set of simultaneous equations is solved by Newton-Raphson iteration. The computer code executes the solution by means of a front-type solver that assembles a portion of the matrix and solves it before assembling the next portion of the matrix. The front solver's efficiency is largely independent of bandwidth and thus does not require as much care in formation of the computational mesh as do traditional solvers.

5. The code RMA-2V is based on the earlier version RMA-2 (Norton and King 1977) but differs from it in several ways. First, it is formulated in

---

* All references cited in this appendix are listed in the References at the end of the main text.

terms of velocity (v) instead of unit discharge (vh), which improves some aspects of the code's behavior; it permits drying and wetting of areas within the grid; and it permits specification of turbulent exchange coefficients in directions other than along the x- and z-axis.

APPENDIX C: THE SEDIMENT TRANSPORT MODEL, STUDH

1. The generalized computer program STUDH solves the depth-integrated convection-dispersion equation in two horizontal dimensions for a single sediment constituent. The form of the solved equation is

$$\frac{\partial C}{\partial t} + u \frac{\partial C}{\partial x} + w \frac{\partial C}{\partial z} = \frac{\partial}{\partial x}\left(D_x \frac{\partial C}{\partial x}\right) + \frac{\partial}{\partial z}\left(D_z \frac{\partial C}{\partial z}\right) + \alpha_1 C + \alpha_2 \qquad \text{(C1)}$$

where

C = concentration, kg/m^3

t = time, sec

u = flow velocity in x-direction, m/sec

x = primary flow direction, m

w = flow velocity in z-direction, m/sec

z = direction perpendicular to x, m

D_x = effective diffusion coefficient in x-direction, m^2/sec

D_z = effective diffusion coefficient in z-direction, m^2/sec

α_1 = coefficient for the source term, 1/sec

α_2 = equilibrium concentration portion of the source term, $kg/m^3/sec$

STUDH is related to the generalized computer program SEDIMENT II (Ariathurai, MacArthur, and Krone 1977)* developed at the University of California, Davis, under the direction of R. B. Krone. STUDH is the product of joint efforts of WES personnel (under the direction of W. A. Thomas) and R. Ariathurai (Resource Management Associates).

2. The source/sink terms in Equation C1 are computed in routines that treat the interaction of the flow and the bed. Separate sections of the code handle computations for clay bed and sand bed problems. In the tests described here, only clay beds were considered. Equation C1 is solved by the finite element method using Galerkin weighted residuals. Like RMA-2V, which uses the same general solution technique, elements are quadrilateral and may have parabolic sides. Shape functions are quadratic. Integration in space is Gaussian. Time-stepping is performed by a Crank-Nicholson approach with a

---

* All references cited in this appendix are listed in the References at the end of the main text.

weighting factor (theta) of 0.66. The solution is fully implicit and a front-type solver is used similar to that in RMA-2V.

3. Several options are available for computing bed shear stress, τ_b, using

$$\tau_b = \rho u_*^2 \tag{C2}$$

where

ρ = water density

u_* = shear velocity

The Manning form of the shear stress equation was used in this study

$$u_* = \frac{un\left(g^{1/2}\right)}{CME\left(D^{1/6}\right)} \tag{C3}$$

where

u = flow velocity

n = Manning's roughness value

g = acceleration due to gravity

CME = coefficient of 1 for SI units and 1.486 for non-SI units

D = flow depth

4. Deposition rates for clay beds were calculated with the equations of Krone (1962):

$$S = \begin{cases} \dfrac{-2V_s}{D} C \left(1 - \dfrac{\tau_b}{\tau_d}\right) \text{ for } C < C_c & \text{(C4)} \\ \dfrac{-2V_k}{D} C^{5/3} \left(1 - \dfrac{\tau_b}{\tau_d}\right) \text{ for } C > C_c & \text{(C5)} \end{cases}$$

where

V_s = fall velocity of a single particle

τ_d = critical shear stress for deposition

C_c = critical concentration = 300 mg/ℓ

$V_k = V_s/C_c^{4/3}$

5. Erosion rates were computed by a simplification of Partheniades (1962) for particle-by-particle erosion. The source term was computed by

$$S = \frac{P}{D}\left(\frac{\tau_b}{\tau_e} - 1\right) \tag{C6}$$

where

P = erosion rate constant

τ_e = critical shear stress for particle erosion